Hindawi Publishing Corporation
Mathematical Problems in Engineering
Volume 2013, Article ID 418374, 26 pages
http://dx.doi.org/10.1155/2013/418374

Research Article

Vibration, Stability, and Resonance of Angle-Ply Composite Laminated Rectangular Thin Plate under Multiexcitations

M. Sayed[1,2] and A. A. Mousa[1,3]

[1] *Department of Mathematics and Statistics, Faculty of Science, Taif University, P.O. Box 888, Al-Taif, Saudi Arabia*
[2] *Department of Engineering Mathematics, Faculty of Electronic Engineering, Menoufia University, Menouf, Egypt*
[3] *Department of Basic Engineering Sciences, Faculty of Engineering, Menoufia University, Shibin El-Kom, Egypt*

Correspondence should be addressed to M. Sayed; moh_6_11@yahoo.com

Received 10 November 2012; Revised 15 April 2013; Accepted 1 May 2013

Academic Editor: Dane Quinn

An analytical investigation of the nonlinear vibration of a symmetric cross-ply composite laminated piezoelectric rectangular plate under parametric and external excitations is presented. The method of multiple time scale perturbation is applied to solve the nonlinear differential equations describing the system up to and including the second-order approximation. All possible resonance cases are extracted at this approximation order. The case of 1 : 1 : 3 primary and internal resonance, where $\Omega_3 \cong \omega_1$, $\omega_2 \cong \omega_1$, and $\omega_3 \cong 3\omega_1$, is considered. The stability of the system is investigated using both phase-plane method and frequency response curves. The influences of the cubic terms on nonlinear dynamic characteristics of the composite laminated piezoelectric rectangular plate are studied. The analytical results given by the method of multiple time scale is verified by comparison with results from numerical integration of the modal equations. Reliability of the obtained results is verified by comparison between the finite difference method (FDM) and Runge-Kutta method (RKM). It is quite clear that some of the simultaneous resonance cases are undesirable in the design of such system. Such cases should be avoided as working conditions for the system. Variation of the parameters $\mu_1, \mu_2, \alpha_7, \beta_8, \omega_1, \omega_2, f_1, f_2$ leads to multivalued amplitudes and hence to jump phenomena. Some recommendations regarding the different parameters of the system are reported. Comparison with the available published work is reported.

1. Introduction

Composite laminated plates that are widely used in several engineering fields such as machinery, shipbuilding, aircraft, automobiles, robot arm, watercraft-hydropower, and wings of helicopters are made of the angle-ply composite laminated plates. Several researchers have focused their attention on studying the nonlinear dynamics, bifurcations, and chaos of the composite laminated plates.

Internal resonance has been found in many engineering problems in which the natural frequencies of the system are commensurable. Ye et al. [1] investigated the local and global nonlinear dynamics of a parametrically excited symmetric cross-ply composite laminated rectangular thin plate under parametric excitation. The study is focused on the case of 1 : 1 internal resonance and primary parametric resonance. Zhang [2] dealt with the global bifurcations and chaotic dynamics of a parametrically excited, simply supported rectangular thin plate. The method of multiple scales is used to obtain the averaged equations. The case of 1 : 1 internal resonance and primary parametric resonance is considered. Guo et al. [3] studied the nonlinear dynamics of a four-edge simply supported angle-ply composite laminated rectangular thin plate excited by both the in-plane and transverse loads. The asymptotic perturbation method is used to derive the four averaged equations under 1 : 1 internal resonance. Zhang et al. [4] investigated the local and global bifurcations of a parametrically and externally excited simply supported rectangular thin plate under simultaneous transversal and in-plane excitations. The studies are focused on the case of 1 : 1 internal resonance and primary parametric resonance. Tien et al. [5] applied the averaging method and Melnikov technique to study local, global bifurcations and chaos of a two-degrees-of-freedom shallow arch subjected to simple harmonic excitation for case of 1 : 2 internal resonances. Sayed and Mousa [6] investigated the influence of the quadratic and cubic terms on nonlinear dynamic characteristics of the angle-ply composite laminated rectangular plate with parametric and external excitations. Two cases of the subharmonic resonances cases in the presence of 1 : 2 internal resonances are considered. The method of multiple time scale perturbation is applied to solve the nonlinear differential equations describing the system up to and including the second-order approximation. Zhang et al. [7] gave further studies on the nonlinear oscillations and chaotic dynamics of a parametrically excited simply supported symmetric cross-ply laminated composite rectangular thin plate with the geometric nonlinearity and nonlinear damping. Zhang et al. [8] dealt with the nonlinear vibrations and chaotic dynamics of a simply supported orthotropic functionally graded material (FGM) rectangular plate subjected to the in-plane and transverse excitations together with thermal loading in the presence of 1 : 2 : 4 internal resonance, primary parametric resonance, and subharmonic resonance of order 1/2. Zhang et al. [9] investigated the bifurcations and chaotic dynamics of a simply supported symmetric cross-ply composite laminated piezoelectric rectangular plate subject to the transverse, in-plane excitations and the excitation loaded by piezoelectric layers. Zhang and Li [10] analyzed the resonant chaotic motions of a simply supported rectangular thin plate with parametrically and externally excitations using exponential dichotomies and an averaging procedure. Zhang et al. [11] analyzed the chaotic dynamics of a six-dimensional nonlinear system which represents the averaged equation of a composite laminated piezoelectric rectangular plate subjected to the transverse, in-plane excitations and the excitation loaded by piezoelectric layers. The case of 1 : 2 : 4 internal resonances is considered. Zhang and Hao [12] studied the global bifurcations and multipulse chaotic dynamics of the composite laminated piezoelectric rectangular plate by using the improved extended Melnikov method. The multipulse chaotic motions of the system are found by using numerical simulation, which further verifies the result of theoretical analysis. Guo and Zhang [13] studied the nonlinear oscillations and chaotic dynamics for a simply supported symmetric cross-ply composite laminated rectangular thin plate with parametric and forcing excitations. The case of 1 : 2 : 3 internal resonance is considered. The method of multiple scales is employed to obtain the six-dimensional averaged equation. The numerical method is used to investigate the periodic and chaotic motions of the composite laminated rectangular thin plate. Eissa and Sayed [14–16] and Sayed [17] investigated the effects of different active controllers on simple and spring pendulum at the primary resonance via negative velocity feedback or its square or cubic. Sayed and Kamel [18, 19] investigated the effects of different controllers on the vibrating system and the saturation control to reduce vibrations due to rotor blade flapping motion. The stability of the system is investigated using both phase-plane method and frequency response curves. Sayed and Hamed [20] studied the response of a two-degree-of-freedom system with quadratic coupling under parametric and harmonic excitations. The method of multiple scale perturbation technique is applied to solve the nonlinear differential equations and obtain approximate solutions up to and including the second-order approximations. Amer et al. [21] investigated the dynamical system of a twin-tail aircraft, which is described by two coupled second-order nonlinear differential equations having both quadratic and cubic nonlinearities under different controllers. Best active control of the system has been achieved via negative acceleration feedback. The stability of the system is investigated applying both frequency response equations and phase-plane method. Hamed et al. [22] studied the nonlinear dynamic behavior of a string-beam coupled system subjected to external, parametric, and tuned excitations that are presented. The case of 1 : 1 internal resonance between the modes of the beam and string, and the primary and combined resonance for the beam is considered. The method of multiple scales is applied to obtain approximate solutions up to and including the second-order approximations. All resonance cases are extracted and investigated. Stability of the system is studied using frequency response equations and the phase-plane method. Awrejcewicz et al. [23–25] studied the chaotic dynamics of continuous mechanical systems such as flexible plates and shallow shells. The considered problems are solved by the Bubnov-Galerkin, Ritz method with higher approximations, and finite difference method. Convergence and validation of those methods are studied. Awrejcewicz et al. [26] investigated the chaotic vibrations of flexible nonlinear Euler-Bernoulli beams subjected to harmonic load and with various boundary conditions. Reliability of the obtained results is verified by the finite difference method and finite element method with the Bubnov-Galerkin approximation for various boundary conditions and various dynamic regimes.

In this paper, the perturbation method and stability of the composite laminated piezoelectric rectangular plate under simultaneous transverse and in-plane excitations are investigated. The method of multiple scales are applied to obtain the second-order uniform asymptotic solutions. All possible resonance cases are extracted at this approximation order. The study is focused on the case of 1 : 1 : 3 internal resonance and primary resonance. The stability of the system and the effects of different parameters on system behavior have been studied using frequency response curves. Stability is performed of figures by solid and dotted lines. The analytical results given by the method of multiple time scale is verified by comparison with results from numerical integration of the modal equations. It is quite clear that some of the simultaneous resonance cases are undesirable in the design of such system. Such cases should be avoided as working conditions for the system. Some recommendations regarding the different parameters of the system are reported. Comparison with the available published work is reported.

2. Mathematical Analysis

Consider a simply supported four edges composite laminated piezoelectric rectangular plate of lengths a, b and thickness h, as shown in Figure 1. The composite laminated piezoelectric rectangular plate is considered as regular symmetric cross-ply laminates with n layers. A Cartesian coordinate system is

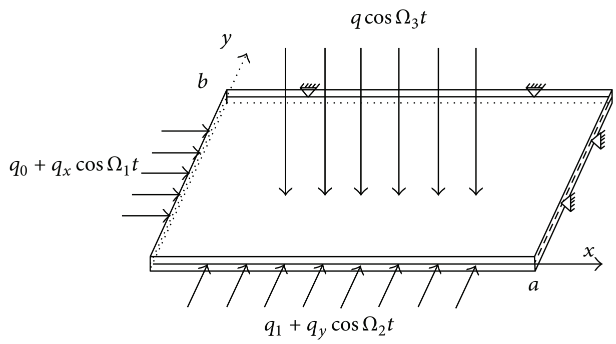

FIGURE 1: The model of the composite laminated piezoelectric rectangular plate.

located in the middle surface of the plate. Assume that u, v, and w represent the displacements of an arbitrary point of the composite laminated piezoelectric rectangular plate in the x, y, and z directions, respectively. The in-plane excitations are loaded along the $y$direction at $x = 0$ in the form $q_0 + q_x\cos\Omega_1 t$, and the excitations are loaded along the x direction at $y = 0$ in the form $q_1 + q_y\cos\Omega_2 t$. The transverse excitation subjected to the composite laminated piezoelectric rectangular plate is represented by $q\cos\Omega_3 t$. The dynamic electrical loading is expressed as $E_z\cos\Omega_4 t$. Based on Reddy's third-order shear deformation plate theory [27], the displacement field at an arbitrary point in the composite laminated plate is expressed as [13]

$$u(x,y,t) = u_0(x,y,t) + z\varphi_x(x,y,t) - z^3\frac{4}{3h^2}\left(\varphi_x + \frac{\partial w_0}{\partial x}\right), \tag{1a}$$

$$v(x,y,t) = v_0(x,y,t) + z\varphi_y(x,y,t) - z^3\frac{4}{3h^2}\left(\varphi_y + \frac{\partial w_0}{\partial y}\right), \tag{1b}$$

$$w(x,y,t) = w_0(x,y,t), \tag{1c}$$

where u_0, v_0, and w_0 are the original displacement on the midplane of the plate in the $x, y,$ and z directions, respectively. Let φ_x and φ_y represent the midplane rotations of transverse normal about the x and y axes, respectively. From the van Karman-type plate theory and Hamilton's principle, the nonlinear governing equations of motion of the composite laminated piezoelectric rectangular plate are given as follows [12]:

$$\frac{\partial N_{xx}}{\partial x} + \frac{\partial N_{xy}}{\partial y} = I_0\ddot{u}_0 + J_1\ddot{\varphi}_x - \frac{4}{3h^2}I_3\frac{\partial \ddot{w}_0}{\partial x}, \tag{2a}$$

$$\frac{\partial N_{xy}}{\partial x} + \frac{\partial N_{yy}}{\partial y} = I_0\ddot{v}_0 + J_1\ddot{\varphi}_y - \frac{4}{3h^2}I_3\frac{\partial \ddot{w}_0}{\partial y}, \tag{2b}$$

$$\begin{aligned}
&\frac{\partial \overline{Q}_x}{\partial x} + \frac{\partial \overline{Q}_y}{\partial y} + \frac{\partial}{\partial x}\left(N_{xx}\frac{\partial w_0}{\partial x} + N_{xy}\frac{\partial w_0}{\partial y}\right) \\
&\quad + \frac{\partial}{\partial y}\left(N_{xy}\frac{\partial w_0}{\partial x} + N_{yy}\frac{\partial w_0}{\partial y}\right) \\
&\quad + \frac{4}{3h^2}\left(\frac{\partial^2 P_{xx}}{\partial x^2} + 2\frac{\partial^2 P_{xy}}{\partial x\partial y} + \frac{\partial^2 P_{yy}}{\partial y^2}\right) + q \\
&= I_0\ddot{w}_0 - \frac{16}{9h^4}I_6\left(\frac{\partial^2 \ddot{w}_0}{\partial x^2} + \frac{\partial^2 \ddot{w}_0}{\partial y^2}\right) \\
&\quad + \frac{4}{3h^2}\left[I_3\left(\frac{\partial \ddot{u}_0}{\partial x} + \frac{\partial \ddot{v}_0}{\partial y}\right) + J_4\left(\frac{\partial \ddot{\varphi}_x}{\partial x} + \frac{\partial \ddot{\varphi}_y}{\partial y}\right)\right],
\end{aligned} \tag{2c}$$

$$\frac{\partial \overline{M}_{xx}}{\partial x} + \frac{\partial \overline{M}_{xy}}{\partial y} - \overline{Q}_x = J_1\ddot{u}_0 + k_2\ddot{\varphi}_x - \frac{4}{3h^2}J_4\frac{\partial \ddot{w}_0}{\partial x}, \tag{2d}$$

$$\frac{\partial \overline{M}_{xy}}{\partial x} + \frac{\partial \overline{M}_{yy}}{\partial y} - \overline{Q}_y = J_1\ddot{v}_0 + k_2\ddot{\varphi}_y - \frac{4}{3h^2}J_4\frac{\partial \ddot{w}_0}{\partial y}. \tag{2e}$$

The boundary conditions of the simply supported rectangular composite laminated plate are expressed as follows:

$$\begin{gathered}
\text{at } x = 0, \quad x = a: \frac{\partial u}{\partial x} = 0, \\
w = u = \varphi_x = \varphi_y = M_{xx} = N_{xy} = \overline{Q}_x = 0,
\end{gathered} \tag{3a}$$

$$\begin{gathered}
\text{at } y = 0, \quad y = b: \frac{\partial v}{\partial y} = 0, \\
w = v = N_{xy} = M_{yy} = \overline{Q}_y = 0,
\end{gathered} \tag{3b}$$

$$\int_0^b N_{xx}\big|_{x=0,\,a}dy = \int_0^b \left(q_0 + q_x\cos\Omega_1 t\right)dy, \tag{3c}$$

$$\int_0^a N_{yy}\big|_{y=0,\,b}dx = \int_0^a \left(q_1 + q_y\cos\Omega_2 t\right)dx. \tag{3d}$$

Applying the Galerkin procedure, we obtain that the dimensionless differential equations of motion for the simply supported symmetric cross-ply rectangular thin plate are shown as follows [11, 28]:

$$\begin{aligned}
&\ddot{u}_1 + \mu_1\dot{u}_1 + \omega_1^2 u_1 \\
&\quad + \left(f_{11}\cos\Omega_1 t + f_{12}\cos\Omega_2 t + f_{14}\cos\Omega_4 t\right)u_1 \\
&\quad + \alpha_1 u_1^2 u_2 + \alpha_2 u_1^2 u_3 + \alpha_3 u_2^2 u_1 + \alpha_4 u_2^2 u_3 \\
&\quad + \alpha_5 u_3^2 u_1 + \alpha_6 u_3^2 u_2 + \alpha_7 u_1^3 + \alpha_8 u_2^3 \\
&\quad + \alpha_9 u_3^3 + \alpha_{10} u_1 u_2 u_3 \\
&= f_1\cos\Omega_3 t,
\end{aligned} \tag{4a}$$

$$\begin{aligned}
&\ddot{u}_2 + \mu_2\dot{u}_2 + \omega_2^2 u_2 \\
&\quad + \left(f_{21}\cos\Omega_1 t + f_{22}\cos\Omega_2 t + f_{24}\cos\Omega_4 t\right) u_2 \\
&\quad + \beta_1 u_1^2 u_2 + \beta_2 u_1^2 u_3 + \beta_3 u_2^2 u_1 + \beta_4 u_2^2 u_3 \\
&\quad + \beta_5 u_3^2 u_1 + \beta_6 u_3^2 u_2 + \beta_7 u_1^3 + \beta_8 u_2^3 \\
&\quad + \beta_9 u_3^3 + \beta_{10} u_1 u_2 u_3 \\
&= f_2 \cos\Omega_3 t,
\end{aligned} \tag{4b}$$

$$\begin{aligned}
&\ddot{u}_3 + \mu_3\dot{u}_3 + \omega_3^2 u_3 \\
&\quad + \left(f_{31}\cos\Omega_1 t + f_{32}\cos\Omega_2 t + f_{34}\cos\Omega_4 t\right) u_3 \\
&\quad + \gamma_1 u_1^2 u_2 + \gamma_2 u_1^2 u_3 + \gamma_3 u_2^2 u_1 + \gamma_4 u_2^2 u_3 \\
&\quad + \gamma_5 u_3^2 u_1 + \gamma_6 u_3^2 u_2 + \gamma_7 u_1^3 + \gamma_8 u_2^3 \\
&\quad + \gamma_9 u_3^3 + \gamma_{10} u_1 u_2 u_3 \\
&= f_3 \cos\Omega_3 t,
\end{aligned} \tag{4c}$$

where u_1, u_2, and u_3 are the vibration amplitudes of the composite laminated piezoelectric rectangular plate for the first-order, second-order, and the third-order modes, respectively, μ_1, μ_2, and μ_3 are the linear viscous damping coefficients, ω_1, ω_2, and ω_3 are the natural frequencies of the rectangular plate, and $\Omega_1, \Omega_2, \Omega_3$, and Ω_4 are the excitations frequencies. f_{n1}, f_{n2}, f_{n3}, and f_n $(n = 1, 2, 3)$ are the amplitudes of parametric and external excitation forces corresponding to the three nonlinear modes, and α_i, β_i, and γ_i $(i = 1, 2, \ldots, 10)$ are the nonlinear coefficients. The linear viscous damping and exciting forces are assumed to be

$$\begin{aligned}
&\mu_n = \varepsilon\hat{\mu}_n, \quad f_{n1} = \varepsilon\hat{f}_{n1}, \quad f_{n2} = \varepsilon\hat{f}_{n2}, \\
&f_{n3} = \varepsilon\hat{f}_{n3}, \quad f_n = \varepsilon^2\hat{f}_n, \quad n = 1, 2, 3,
\end{aligned} \tag{5}$$

where ε is a small perturbation parameter and $0 < \varepsilon \ll 1$.

The external excitation forces $\hat{f}_n$ are of the order 2, and the linear viscous damping $\hat{\mu}_n$, parametric exciting forces $\hat{f}_{n1}$, $\hat{f}_{n2}$, and $\hat{f}_{n3}$ are of the order 1.

To consider the influence of the cubic terms on nonlinear dynamic characteristics of the composite laminated piezoelectric rectangular plate, we need to obtain the second-order approximate solution of (4a), (4b), and (4c). Method of multiple scales [29–31] is applied to obtain a second-order approximation for the system. For the second-order approximation, we introduce three time scales defined by

$$T_0 = t, \qquad T_1 = \varepsilon t, \qquad T_2 = \varepsilon^2 t. \tag{6}$$

In terms of these scales, the time derivatives become

$$\frac{d}{dt} = D_0 + \varepsilon D_1 + \varepsilon^2 D_2, \tag{7a}$$

$$\frac{d^2}{dt^2} = D_0^2 + 2\varepsilon D_0 D_1 + \varepsilon^2\left(D_1^2 + 2D_0 D_2\right), \tag{7b}$$

where $D_n = \partial/\partial T_n$, $n = 0, 1, 2$. We seek a uniform approximation to the solution of (4a), (4b), and (4c) in the form:

$$\begin{aligned}
u_n(t,\varepsilon) &= \varepsilon u_{n1}\left(T_0, T_1, T_2\right) + \varepsilon^2 u_{n2}\left(T_0, T_1, T_2\right) \\
&\quad + \varepsilon^3 u_{n3}\left(T_0, T_1, T_2\right) + O\left(\varepsilon^4\right), \quad n = 1, 2, 3.
\end{aligned} \tag{8}$$

Terms of $O(\varepsilon^4)$ and higher orders are neglected. Substituting (5) and (7a)–(8) into (4a), (4b), and (4c) and equating the coefficients of like powers of ε, we obtain the following.

Order ε

$$\left(D_0^2 + \omega_1^2\right) u_{11} = 0, \tag{9a}$$

$$\left(D_0^2 + \omega_2^2\right) u_{21} = 0, \tag{9b}$$

$$\left(D_0^2 + \omega_3^2\right) u_{31} = 0. \tag{9c}$$

Order ε^2

$$\begin{aligned}
\left(D_0^2 + \omega_1^2\right) u_{12} &= -2D_0 D_1 u_{11} - \hat{\mu}_1 D_0 u_{11} \\
&\quad - \left(\hat{f}_{11}\cos\Omega_1 T_0 + \hat{f}_{12}\cos\Omega_2 T_0\right. \\
&\quad \left. + \hat{f}_{14}\cos\Omega_4 T_0\right) u_{11} + \hat{f}_1 \cos\Omega_3 T_0,
\end{aligned} \tag{10a}$$

$$\begin{aligned}
\left(D_0^2 + \omega_2^2\right) u_{22} &= -2D_0 D_1 u_{21} - \hat{\mu}_2 D_0 u_{21} \\
&\quad - \left(\hat{f}_{21}\cos\Omega_1 T_0 + \hat{f}_{22}\cos\Omega_2 T_0\right. \\
&\quad \left. + \hat{f}_{24}\cos\Omega_4 T_0\right) u_{21} + \hat{f}_2 \cos\Omega_3 T_0,
\end{aligned} \tag{10b}$$

$$\begin{aligned}
\left(D_0^2 + \omega_3^2\right) u_{32} &= -2D_0 D_1 u_{31} - \hat{\mu}_3 D_0 u_{31} \\
&\quad - \left(\hat{f}_{31}\cos\Omega_1 T_0 + \hat{f}_{32}\cos\Omega_2 T_0\right. \\
&\quad \left. + \hat{f}_{34}\cos\Omega_4 T_0\right) u_{31} + \hat{f}_3 \cos\Omega_3 T_0.
\end{aligned} \tag{10c}$$

Order ε^3

$$\begin{aligned}
\left(D_0^2 + \omega_1^2\right) u_{13} &= -D_1^2 u_{11} - 2D_0 D_2 u_{11} - 2D_0 D_1 u_{12} \\
&\quad - \hat{\mu}_1\left(D_0 u_{12} + D_1 u_{11}\right) \\
&\quad - \left(\hat{f}_{11}\cos\Omega_1 T_0 + \hat{f}_{12}\cos\Omega_2 T_0\right. \\
&\quad \left. + \hat{f}_{14}\cos\Omega_4 T_0\right) u_{12} \\
&\quad - \alpha_1 u_{11}^2 u_{21} - \alpha_2 u_{11}^2 u_{31} - \alpha_3 u_{21}^2 u_{11} \\
&\quad - \alpha_4 u_{21}^2 u_{31} - \alpha_5 u_{31}^2 u_{11} - \alpha_6 u_{31}^2 u_{21} \\
&\quad - \alpha_7 u_{11}^3 - \alpha_8 u_{21}^3 - \alpha_9 u_{31}^3 - \alpha_{10} u_{11} u_{21} u_{31},
\end{aligned} \tag{11a}$$

$$\begin{aligned}\left(D_0^2+\omega_2^2\right)u_{23} = {} & -D_1^2u_{21}-2D_0D_2u_{21}-2D_0D_1u_{22} \\ & -\widehat{\mu}_2\left(D_0u_{22}+D_1u_{21}\right) \\ & -\left(\widehat{f}_{21}\cos\Omega_1T_0+\widehat{f}_{22}\cos\Omega_2T_0\right. \\ & \quad \left.+\widehat{f}_{24}\cos\Omega_4T_0\right)u_{22} \\ & -\beta_1u_{11}^2u_{21}-\beta_2u_{11}^2u_{31}-\beta_3u_{21}^2u_{11} \\ & -\beta_4u_{21}^2u_{31}-\beta_5u_{31}^2u_{11}-\beta_6u_{31}^2u_{21} \\ & -\beta_7u_{11}^3-\beta_8u_{21}^3-\beta_9u_{31}^3-\beta_{10}u_{11}u_{21}u_{31},\end{aligned} \tag{11b}$$

$$\begin{aligned}\left(D_0^2+\omega_3^2\right)u_{33} = {} & -D_1^2u_{31}-2D_0D_2u_{31}-2D_0D_1u_{32} \\ & -\widehat{\mu}_3\left(D_0u_{32}+D_1u_{31}\right) \\ & -\left(\widehat{f}_{31}\cos\Omega_1T_0+\widehat{f}_{32}\cos\Omega_2T_0\right. \\ & \quad \left.+\widehat{f}_{34}\cos\Omega_4T_0\right)u_{32} \\ & -\gamma_1u_{11}^2u_{21}-\gamma_2u_{11}^2u_{31}-\gamma_3u_{21}^2u_{11} \\ & -\gamma_4u_{21}^2u_{31}-\gamma_5u_{31}^2u_{11}-\gamma_6u_{31}^2u_{21} \\ & -\gamma_7u_{11}^3-\gamma_8u_{21}^3-\gamma_9u_{31}^3-\gamma_{10}u_{11}u_{21}u_{31}.\end{aligned} \tag{11c}$$

The general solutions of (9a), (9b), and (9c) can be written in the form

$$u_{11} = A_1\left(T_1,T_2\right)\exp\left(i\omega_1T_0\right)+cc, \tag{12a}$$

$$u_{21} = A_2\left(T_1,T_2\right)\exp\left(i\omega_2T_0\right)+cc, \tag{12b}$$

$$u_{31} = A_3\left(T_1,T_2\right)\exp\left(i\omega_3T_0\right)+cc, \tag{12c}$$

where A_1, A_2, and A_3 are a complex function in T_1, T_2 which can be determined from eliminating the secular terms at the next approximation and cc stands for the complex conjugate of the preceding terms. Substituting (12a), (12b), and (12c) into (10a), (10b), and (10c) and eliminating the secular terms, then the first-order approximations are given by

$$\begin{aligned}u_{12} = {} & E_1\exp\left(i\omega_1T_0\right)+E_2\exp\left(i\left(\Omega_1+\omega_1\right)T_0\right) \\ & +E_3\exp\left(i\left(\Omega_1-\omega_1\right)T_0\right)+E_4\exp\left(i\left(\Omega_2+\omega_1\right)T_0\right) \\ & +E_5\exp\left(i\left(\Omega_2-\omega_1\right)T_0\right)+E_6\exp\left(i\left(\Omega_4+\omega_1\right)T_0\right) \\ & +E_7\exp\left(i\left(\Omega_4-\omega_1\right)T_0\right)+cc,\end{aligned} \tag{13a}$$

$$\begin{aligned}u_{22} = {} & E_8\exp\left(i\omega_2T_0\right)+E_9\exp\left(i\left(\Omega_1+\omega_2\right)T_0\right) \\ & +E_{10}\exp\left(i\left(\Omega_1-\omega_2\right)T_0\right)+E_{11}\exp\left(i\left(\Omega_2+\omega_2\right)T_0\right) \\ & +E_{12}\exp\left(i\left(\Omega_2-\omega_2\right)T_0\right)+E_{13}\exp\left(i\left(\Omega_4+\omega_2\right)T_0\right) \\ & +E_{14}\exp\left(i\left(\Omega_4-\omega_2\right)T_0\right)+cc,\end{aligned} \tag{13b}$$

$$\begin{aligned}u_{32} = {} & E_{15}\exp\left(i\omega_3T_0\right)+E_{16}\exp\left(i\left(\Omega_1+\omega_3\right)T_0\right) \\ & +E_{17}\exp\left(i\left(\Omega_1-\omega_3\right)T_0\right)+E_{18}\exp\left(i\left(\Omega_2+\omega_3\right)T_0\right) \\ & +E_{19}\exp\left(i\left(\Omega_2-\omega_3\right)T_0\right)+E_{20}\exp\left(i\left(\Omega_4+\omega_3\right)T_0\right) \\ & +E_{21}\exp\left(i\left(\Omega_4-\omega_3\right)T_0\right)+E_{22}\exp\left(i\Omega_3T_0\right)+cc,\end{aligned} \tag{13c}$$

where E_i ($i = 1, 2, \ldots, 22$) are the complex functions in T_1 and T_2. From (12a)–(13c) into (11a), (11b), and (11c) and eliminating the secular terms, the second-order approximation is given by

$$\begin{aligned}u_{13}\left(T_0,T_1,T_2\right) = {} & H_1\exp\left(i\omega_2T_0\right)+H_2\exp\left(i\omega_3T_0\right) \\ & +H_3\exp\left(3i\omega_1T_0\right)+H_4\exp\left(3i\omega_2T_0\right) \\ & +H_5\exp\left(3i\omega_3T_0\right) \\ & +H_6\exp\left(i\left(\omega_2\pm2\omega_1\right)T_0\right) \\ & +H_7\exp\left(i\left(\omega_3\pm2\omega_1\right)T_0\right) \\ & +H_8\exp\left(i\left(2\omega_2\pm\omega_1\right)T_0\right) \\ & +H_9\exp\left(i\left(2\omega_3\pm\omega_1\right)T_0\right) \\ & +H_{10}\exp\left(i\left(\omega_2\pm2\omega_3\right)T_0\right) \\ & +H_{11}\exp\left(i\left(\omega_3\pm2\omega_2\right)T_0\right) \\ & +H_{12}\exp\left(i\left(\omega_3\pm\omega_2\pm\omega_1\right)T_0\right) \\ & +H_{13}\exp\left(i\Omega_3T_0\right) \\ & +H_{14}\exp\left(i\left(\Omega_3\pm\Omega_1\right)T_0\right) \\ & +H_{15}\exp\left(i\left(\Omega_3\pm\Omega_2\right)T_0\right) \\ & +H_{16}\exp\left(i\left(\Omega_3\pm\Omega_4\right)T_0\right) \\ & +H_{17}\exp\left(i\left(\Omega_1\pm\omega_1\right)T_0\right) \\ & +H_{18}\exp\left(i\left(\Omega_2\pm\omega_1\right)T_0\right) \\ & +H_{19}\exp\left(i\left(\Omega_4\pm\omega_1\right)T_0\right) \\ & +H_{20}\exp\left(i\left(2\Omega_1\pm\omega_1\right)T_0\right) \\ & +H_{21}\exp\left(i\left(2\Omega_2\pm\omega_1\right)T_0\right) \\ & +H_{22}\exp\left(i\left(2\Omega_4\pm\omega_1\right)T_0\right) \\ & +H_{23}\exp\left(i\left(\Omega_2\pm\Omega_1\pm\omega_1\right)T_0\right) \\ & +H_{24}\exp\left(i\left(\Omega_4\pm\Omega_1\pm\omega_1\right)T_0\right) \\ & +H_{25}\exp\left(i\left(\Omega_4\pm\Omega_2\pm\omega_1\right)T_0\right)+cc,\end{aligned} \tag{14a}$$

$$\begin{aligned}u_{23}\left(T_0,T_1,T_2\right) = {} & H_{26}\exp\left(i\omega_1T_0\right)+H_{27}\exp\left(i\omega_3T_0\right) \\ & +H_{28}\exp\left(3i\omega_1T_0\right)+H_{29}\exp\left(3i\omega_2T_0\right)\end{aligned}$$

$$
\begin{aligned}
&+ H_{30} \exp\left(3i\omega_3 T_0\right) \\
&+ H_{31} \exp\left(i\left(\omega_2 \pm 2\omega_1\right) T_0\right) \\
&+ H_{32} \exp\left(i\left(2\omega_2 \pm \omega_1\right) T_0\right) \\
&+ H_{33} \exp\left(i\left(\omega_3 \pm 2\omega_1\right) T_0\right) \\
&+ H_{34} \exp\left(i\left(2\omega_3 \pm \omega_1\right) T_0\right) \\
&+ H_{35} \exp\left(i\left(\omega_2 \pm 2\omega_3\right) T_0\right) \\
&+ H_{36} \exp\left(i\left(2\omega_2 \pm \omega_3\right) T_0\right) \\
&+ H_{37} \exp\left(i\left(\omega_3 \pm \omega_2 \pm \omega_1\right) T_0\right) \\
&+ H_{38} \exp\left(i\Omega_3 T_0\right) \\
&+ H_{39} \exp\left(i\left(\Omega_3 \pm \Omega_1\right) T_0\right) \\
&+ H_{40} \exp\left(i\left(\Omega_3 \pm \Omega_2\right) T_0\right) \\
&+ H_{41} \exp\left(i\left(\Omega_4 \pm \Omega_3\right) T_0\right) \\
&+ H_{42} \exp\left(i\left(\Omega_1 \pm \omega_2\right) T_0\right) \\
&+ H_{43} \exp\left(i\left(\Omega_2 \pm \omega_2\right) T_0\right) \\
&+ H_{44} \exp\left(i\left(\Omega_4 \pm \omega_2\right) T_0\right) \\
&+ H_{45} \exp\left(i\left(2\Omega_1 \pm \omega_2\right) T_0\right) \\
&+ H_{46} \exp\left(i\left(2\Omega_2 \pm \omega_2\right) T_0\right) \\
&+ H_{47} \exp\left(i\left(2\Omega_4 \pm \omega_2\right) T_0\right) \\
&+ H_{48} \exp\left(i\left(\Omega_2 \pm \Omega_1 \pm \omega_2\right) T_0\right) \\
&+ H_{49} \exp\left(i\left(\Omega_4 \pm \Omega_1 \pm \omega_2\right) T_0\right) \\
&+ H_{50} \exp\left(i\left(\Omega_4 \pm \Omega_2 \pm \omega_2\right) T_0\right) + cc,
\end{aligned} \tag{14b}
$$

$$
\begin{aligned}
u_{33}\left(T_0, T_1, T_2\right) = {} & H_{51} \exp\left(3i\omega_3 T_0\right) + H_{52} \exp\left(i\omega_1 T_0\right) \\
&+ H_{53} \exp\left(3i\omega_1 T_0\right) + H_{54} \exp\left(i\omega_2 T_0\right) \\
&+ H_{55} \exp\left(3i\omega_2 T_0\right) \\
&+ H_{56} \exp\left(i\left(\omega_2 \pm 2\omega_1\right) T_0\right) \\
&+ H_{57} \exp\left(i\left(2\omega_2 \pm \omega_1\right) T_0\right) \\
&+ H_{58} \exp\left(i\left(\omega_3 \pm 2\omega_1\right) T_0\right) \\
&+ H_{59} \exp\left(i\left(2\omega_3 \pm \omega_1\right) T_0\right) \\
&+ H_{60} \exp\left(i\left(\omega_2 \pm 2\omega_3\right) T_0\right) \\
&+ H_{61} \exp\left(i\left(2\omega_2 \pm \omega_3\right) T_0\right) \\
&+ H_{62} \exp\left(i\left(\omega_3 \pm \omega_2 \pm \omega_1\right) T_0\right) \\
&+ H_{63} \exp\left(i\Omega_3 T_0\right) \\
&+ H_{64} \exp\left(i\left(\Omega_3 \pm \Omega_1\right) T_0\right) \\
&+ H_{65} \exp\left(i\left(\Omega_3 \pm \Omega_2\right) T_0\right) \\
&+ H_{66} \exp\left(i\left(\Omega_3 \pm \Omega_4\right) T_0\right) \\
&+ H_{67} \exp\left(i\left(\Omega_1 \pm \omega_3\right) T_0\right) \\
&+ H_{68} \exp\left(i\left(\Omega_2 \pm \omega_3\right) T_0\right) \\
&+ H_{69} \exp\left(i\left(\Omega_4 \pm \omega_3\right) T_0\right) \\
&+ H_{70} \exp\left(i\left(2\Omega_1 \pm \omega_3\right) T_0\right) \\
&+ H_{71} \exp\left(i\left(2\Omega_2 \pm \omega_3\right) T_0\right) \\
&+ H_{72} \exp\left(i\left(2\Omega_4 \pm \omega_3\right) T_0\right) \\
&+ H_{73} \exp\left(i\left(\Omega_2 \pm \Omega_1 \pm \omega_3\right) T_0\right) \\
&+ H_{74} \exp\left(i\left(\Omega_4 \pm \Omega_1 \pm \omega_3\right) T_0\right) \\
&+ H_{75} \exp\left(i\left(\Omega_4 \pm \Omega_2 \pm \omega_3\right) T_0\right) + cc,
\end{aligned} \tag{14c}
$$

where H_i ($i = 1, 2, \ldots, 75$) are the complex functions in T_1 and T_2. From the above derived solutions, the reported resonance cases are the following.

(i) *Primary resonance*: $\Omega_1 \cong \omega_n$, $\Omega_2 \cong \omega_n$, $\Omega_3 \cong \omega_n$, $\Omega_4 \cong \omega_n$, and $n = 1, 2, 3$.

(ii) *Subharmonic resonance*: $\Omega_1 \cong 2\omega_n$, $\Omega_2 \cong 2\omega_n$, $\Omega_4 \cong 2\omega_n$, and $n = 1, 2, 3$.

(iii) *Internal or secondary resonance*: $\omega_1 \cong \omega_2$, $\omega_2 \cong \omega_3$, $\omega_3 \cong \omega_1$, $\omega_1 \cong 3\omega_s$, $\omega_2 \cong 3\omega_r$, $\omega_3 \cong 3\omega_m$, $s = 2, 3$, $r = 1, 3$, and $m = 1, 2$.

(iv) *Combined resonance*: $\omega_3 \pm \omega_2 \cong 2\omega_1$, $\omega_3 \pm \omega_1 \cong 2\omega_2$, $\omega_1 \pm \omega_2 \cong 2\omega_3$, $\omega_2 \pm 2\omega_3 \cong \omega_1$, $\omega_3 \pm 2\omega_2 \cong \omega_1$, $\omega_3 \pm 2\omega_1 \cong \omega_2$, $\omega_1 \pm 2\omega_3 \cong \omega_2$, $\omega_2 \pm 2\omega_1 \cong \omega_3$, $\omega_1 \pm 2\omega_2 \cong \omega_3$, $\Omega_3 \pm \Omega_t \cong \omega_n$, $\Omega_4 \pm \Omega_m \cong 2\omega_n$, $\Omega_2 \pm \Omega_1 \cong 2\omega_n$, $t = 1, 2, 4$, $m = 1, 2$, and $n = 1, 2, 3$.

(v) *Simultaneous or incident resonance*.

Any combination of the previous resonance cases is considered as simultaneous resonance.

3. Stability Analysis

The behavior of such a system can be very complex, especially when the natural frequencies and the forcing frequency satisfy certain internal and external resonance conditions. The study is focused on the case of 1 : 1 : 3 primary resonance and internal resonance, where $\Omega_3 \cong \omega_1$, $\omega_2 \cong \omega_1$, and $\omega_3 \cong 3\omega_1$. To describe how close the frequencies are to the resonance conditions, we introduce detuning parameters as follows:

$$
\begin{aligned}
\Omega_3 &= \omega_1 + \sigma_1 = \omega_1 + \varepsilon\hat{\sigma}_1, \\
\omega_2 &= \omega_1 + \sigma_2 = \omega_1 + \varepsilon\hat{\sigma}_2, \\
\omega_3 &= 3\omega_1 + \sigma_3 = 3\omega_1 + \varepsilon\hat{\sigma}_3,
\end{aligned} \tag{15}
$$

where σ_1 and σ_2, σ_3 are called the external and internal detuning parameters, respectively. Eliminating the secular terms leads to solvability conditions for the first- and second-order expansions as follows:

$$2i\omega_1 D_1 A_1 = -i\widehat{\mu}_1\omega_1 A_1 + \frac{\widehat{f}_1}{2}\exp\left(i\widehat{\sigma}_1 T_1\right), \tag{16a}$$

$$2i\omega_2 D_1 A_2 = -i\widehat{\mu}_2\omega_2 A_2 + \frac{\widehat{f}_2}{2}\exp\left(i\left(\widehat{\sigma}_1 - \widehat{\sigma}_2\right)T_1\right), \tag{16b}$$

$$2i\omega_3 D_1 A_3 = -i\widehat{\mu}_3\omega_3 A_3, \tag{16c}$$

$$\begin{aligned}
&2i\omega_1 D_2 A_1 \\
&= -D_1^2 A_1 - \widehat{\mu}_1 D_1 A_1 \\
&\quad - \left\{\frac{\widehat{f}_{11}^2}{2\left(\Omega_1^2 - 4\omega_1^2\right)} + \frac{\widehat{f}_{12}^2}{2\left(\Omega_2^2 - 4\omega_1^2\right)} + \frac{\widehat{f}_{14}^2}{2\left(\Omega_4^2 - 4\omega_1^2\right)}\right\} A_1 \\
&\quad - \left\{2\alpha_1 A_1\overline{A}_1 + 2\alpha_6 A_3\overline{A}_3 + 3\alpha_8 A_2\overline{A}_2\right\} A_2 \exp\left(i\widehat{\sigma}_2 T_1\right) \\
&\quad - \alpha_1 A_1^2\overline{A}_2 \exp\left(-i\widehat{\sigma}_2 T_1\right) - \alpha_2 \overline{A}_1^2 A_3 \exp\left(i\widehat{\sigma}_3 T_1\right) \\
&\quad - \left\{2\alpha_3 A_2\overline{A}_2 + 2\alpha_5 A_3\overline{A}_3 + 3\alpha_7 A_1\overline{A}_1\right\} A_1 \\
&\quad - \alpha_4 \overline{A}_2^2 A_3 \exp\left(i\left(\widehat{\sigma}_3 - 2\widehat{\sigma}_2\right)T_1\right) \\
&\quad - \alpha_{10}\overline{A}_1\overline{A}_2 A_3 \exp\left(i\left(\widehat{\sigma}_3 - \widehat{\sigma}_2\right)T_1\right),
\end{aligned} \tag{17a}$$

$$\begin{aligned}
&2i\omega_2 D_2 A_2 \\
&= -D_1^2 A_2 - \widehat{\mu}_2 D_1 A_2 \\
&\quad - \left\{\frac{\widehat{f}_{21}^2}{2\left(\Omega_1^2 - 4\omega_2^2\right)} + \frac{\widehat{f}_{22}^2}{2\left(\Omega_2^2 - 4\omega_2^2\right)} + \frac{\widehat{f}_{24}^2}{2\left(\Omega_4^2 - 4\omega_2^2\right)}\right\} A_2 \\
&\quad - \left\{2\beta_3 A_2\overline{A}_2 + 2\beta_5 A_3\overline{A}_3 + 3\beta_7 A_1\overline{A}_1\right\} \\
&\quad \times A_1 \exp\left(-i\widehat{\sigma}_2 T_1\right) \\
&\quad - \beta_3 A_2^2\overline{A}_1 \exp\left(i\widehat{\sigma}_2 T_1\right) - \beta_1 A_1^2\overline{A}_2 \exp\left(-2i\widehat{\sigma}_2 T_1\right) \\
&\quad - \left\{2\beta_6 A_3\overline{A}_3 + 2\beta_1\overline{A}_1 A_1 + 3\beta_8 A_2\overline{A}_2\right\} A_2 \\
&\quad - \beta_2 \overline{A}_1^2 A_3 \exp\left(i\left(\widehat{\sigma}_3 - \widehat{\sigma}_2\right)T_1\right) \\
&\quad - \beta_{10}\overline{A}_1\overline{A}_2 A_3 \exp\left(i\left(\widehat{\sigma}_3 - 2\widehat{\sigma}_2\right)T_1\right) \\
&\quad - \beta_4 \overline{A}_2^2 A_3 \exp\left(i\left(\widehat{\sigma}_3 - 3\widehat{\sigma}_2\right)T_1\right),
\end{aligned} \tag{17b}$$

$$\begin{aligned}
&2i\omega_3 D_2 A_3 \\
&= -D_1^2 A_3 - \widehat{\mu}_3 D_1 A_3 \\
&\quad - \left\{\frac{\widehat{f}_{31}^2}{2\left(\Omega_1^2 - 4\omega_3^2\right)} + \frac{\widehat{f}_{32}^2}{2\left(\Omega_2^2 - 4\omega_3^2\right)} + \frac{\widehat{f}_{34}^2}{2\left(\Omega_4^2 - 4\omega_3^2\right)}\right\} A_3 \\
&\quad - \gamma_{10} A_1\overline{A}_2 A_3 \exp\left(-i\widehat{\sigma}_2 T_1\right) \\
&\quad - \gamma_{10}\overline{A}_1 A_2 A_3 \exp\left(i\widehat{\sigma}_2 T_1\right) \\
&\quad - \gamma_7 A_1^3 \exp\left(-i\widehat{\sigma}_3 T_1\right) \\
&\quad - \left\{2\gamma_2 A_1\overline{A}_1 + 2\gamma_4 A_2\overline{A}_2 + 3\gamma_9 A_3\overline{A}_3\right\} A_3 \\
&\quad - \gamma_1 A_1^2 A_2 \exp\left(i\left(\widehat{\sigma}_2 - \widehat{\sigma}_3\right)T_1\right) \\
&\quad - \gamma_3 A_2^2 A_1 \exp\left(i\left(2\widehat{\sigma}_2 - \widehat{\sigma}_3\right)T_1\right) \\
&\quad - \gamma_8 A_2^3 \exp\left(i\left(3\widehat{\sigma}_2 - \widehat{\sigma}_3\right)T_1\right).
\end{aligned} \tag{17c}$$

From (7a), multiplying both sides by $2i\omega_n$, we get

$$2i\omega_n \frac{dA_n}{dt} = \varepsilon 2i\omega_n D_1 A_n + \varepsilon^2 2i\omega_n D_2 A_n, \quad n = 1, 2, 3. \tag{18}$$

To analyze the solutions of (16a)–(17c), we express A_n in the polar form as follows:

$$\begin{aligned}
A_n\left(T_1, T_2\right) &= \frac{\widehat{a}_n}{2}\exp\left(i\varphi_n\right), \\
a_n &= \varepsilon\widehat{a}_n, \quad (n = 1, 2, 3),
\end{aligned} \tag{19}$$

where a_n and φ_n are the steady-state amplitudes and phases of the motion, respectively. Substituting (16a)–(17c) and (19) into (18) and equating the real and imaginary parts, we obtain the following equations describing the modulation of the amplitudes and phases of the response:

$$\begin{aligned}
\dot{a}_1 = &-\frac{\mu_1}{2}a_1 + \left\{\frac{f_1}{2\omega_1} - \frac{\sigma_1 f_1}{4\omega_1^2}\right\}\sin\theta_1 \\
&+ \frac{\mu_1 f_1}{8\omega_1^2}\cos\theta_1 - \frac{\alpha_1}{8\omega_1}a_1^2 a_2 \sin\theta_2 \\
&- \frac{\alpha_2}{8\omega_1}a_1^2 a_3 \sin\theta_3 - \frac{\alpha_4}{8\omega_1}a_2^2 a_3 \sin\left(\theta_3 - 2\theta_2\right) \\
&- \frac{\alpha_6}{4\omega_1}a_3^2 a_2 \sin\theta_2 - \frac{3\alpha_8}{8\omega_1}a_2^3 \sin\theta_2 \\
&- \frac{\alpha_{10}}{8\omega_1}a_1 a_2 a_3 \sin\left(\theta_3 - \theta_2\right),
\end{aligned}$$

$$\begin{aligned}
a_1\dot{\varphi}_1 = &\left\{-\frac{\mu_1^2}{8\omega_1} + \frac{\Gamma_1}{2\omega_1}\right\}a_1 - \left\{\frac{f_1}{2\omega_1} - \frac{\sigma_1 f_1}{4\omega_1^2}\right\}\cos\theta_1 \\
&+ \frac{\mu_1 f_1}{8\omega_1^2}\sin\theta_1 + \frac{3\alpha_1}{8\omega_1}a_1^2 a_2 \cos\theta_2 + \frac{\alpha_2}{8\omega_1}a_1^2 a_3 \cos\theta_3 \\
&+ \frac{\alpha_3}{4\omega_1}a_1 a_2^2 + \frac{\alpha_4}{8\omega_1}a_2^2 a_3 \cos\left(\theta_3 - 2\theta_2\right) \\
&+ \frac{\alpha_5}{4\omega_1}a_1 a_3^2 + \frac{\alpha_6}{4\omega_1}a_3^2 a_2 \cos\theta_2 + \frac{3\alpha_7}{8\omega_1}a_1^3
\end{aligned}$$

$$
\begin{aligned}
&+\frac{3\alpha_8}{8\omega_1}a_2^3\cos\theta_2+\frac{\alpha_{10}}{8\omega_1}a_1a_2a_3\cos\left(\theta_3-\theta_2\right),\\
\dot{a}_2 &= -\frac{\mu_2}{2}a_2+\left\{\frac{f_2}{2\omega_2}-\frac{\left(\sigma_1-\sigma_2\right)f_2}{4\omega_2^2}\right\}\sin\left(\theta_1-\theta_2\right)\\
&+\frac{\mu_2 f_2}{8\omega_2^2}\cos\left(\theta_1-\theta_2\right)+\frac{\beta_1}{8\omega_2}a_1^2a_2\sin 2\theta_2\\
&-\frac{\beta_2}{8\omega_2}a_1^2a_3\sin\left(\theta_3-\theta_2\right)+\frac{\beta_3}{8\omega_2}a_2^2a_1\sin\theta_2\\
&-\frac{\beta_4}{8\omega_2}a_2^2a_3\sin\left(\theta_3-3\theta_2\right)+\frac{\beta_5}{4\omega_2}a_3^2a_1\sin\theta_2\\
&+\frac{3\beta_7}{8\omega_2}a_1^3\sin\theta_2-\frac{\beta_{10}}{8\omega_2}a_1a_2a_3\sin\left(\theta_3-2\theta_2\right),\\
a_2\dot{\varphi}_2 &= \left\{-\frac{\mu_2^2}{8\omega_2}+\frac{\Gamma_2}{2\omega_2}\right\}a_2\\
&+\left\{\frac{\left(\sigma_1-\sigma_2\right)f_2}{4\omega_2^2}-\frac{f_2}{2\omega_2}\right\}\cos\left(\theta_1-\theta_2\right)\\
&+\frac{\mu_2 f_2}{8\omega_2^2}\sin\left(\theta_1-\theta_2\right)+\frac{\beta_1}{8\omega_2}a_1^2a_2\cos 2\theta_2\\
&+\frac{\beta_1}{4\omega_2}a_1^2a_2+\frac{\beta_2}{8\omega_2}a_1^2a_3\cos\left(\theta_3-\theta_2\right)\\
&+\frac{3\beta_3}{8\omega_2}a_2^2a_1\cos\theta_2+\frac{\beta_4}{8\omega_2}a_2^2a_3\cos\left(\theta_3-3\theta_2\right)\\
&+\frac{\beta_5}{4\omega_2}a_3^2a_1\cos\theta_2+\frac{\beta_6}{4\omega_2}a_3^2a_2+\frac{3\beta_7}{8\omega_2}a_1^3\cos\theta_2\\
&+\frac{3\beta_8}{8\omega_2}a_2^3+\frac{\beta_{10}}{8\omega_2}a_1a_2a_3\cos\left(\theta_3-2\theta_2\right),\\
\dot{a}_3 &= -\frac{\mu_3}{2}a_3-\frac{\gamma_1}{8\omega_3}a_1^2a_2\sin\left(\theta_2-\theta_3\right)\\
&-\frac{\gamma_3}{8\omega_3}a_2^2a_1\sin\left(2\theta_2-\theta_3\right)+\frac{\gamma_7}{8\omega_3}a_1^3\sin\theta_3\\
&-\frac{\gamma_8}{8\omega_3}a_2^3\sin\left(3\theta_2-\theta_3\right),\\
a_3\dot{\varphi}_3 &= \left\{-\frac{\mu_3^2}{8\omega_3}+\frac{\Gamma_3}{2\omega_3}\right\}a_3+\frac{\gamma_1}{8\omega_3}a_1^2a_2\cos\left(\theta_2-\theta_3\right)\\
&+\frac{\gamma_2}{4\omega_3}a_1^2a_3+\frac{\gamma_3}{8\omega_3}a_2^2a_1\cos\left(2\theta_2-\theta_3\right)\\
&+\frac{\gamma_4}{4\omega_3}a_2^2a_3+\frac{\gamma_7}{8\omega_3}a_1^3\cos\theta_3\\
&+\frac{\gamma_8}{8\omega_3}a_2^3\cos\left(3\theta_2-\theta_3\right)+\frac{3\gamma_9}{8\omega_3}a_3^3\\
&+\frac{\gamma_{10}}{4\omega_3}a_1a_2a_3\cos\theta_2,
\end{aligned}
\tag{20}
$$

where

$$
\begin{aligned}
\Gamma_n &= \left\{\frac{f_{n1}^2}{2\left(\Omega_1^2-4\omega_n^2\right)}+\frac{f_{n2}^2}{2\left(\Omega_2^2-4\omega_n^2\right)}+\frac{f_{n4}^2}{2\left(\Omega_4^2-4\omega_n^2\right)}\right\},\\
&\qquad n=1,2,3,\\
\theta_1 &= \hat{\sigma}_1T_1-\varphi_1,\\
\theta_2 &= \hat{\sigma}_2T_1+\varphi_2-\varphi_1,\\
\theta_3 &= \hat{\sigma}_3T_1+\varphi_3-3\varphi_1.
\end{aligned}
\tag{21}
$$

Steady-state solutions of the system correspond to the fixed points of (20), which in turn correspond to

$$
\begin{aligned}
\dot{\varphi}_1 &= \sigma_1,\\
\dot{\varphi}_2 &= \sigma_1-\sigma_2,\\
\dot{\varphi}_3 &= 3\sigma_1-\sigma_3.
\end{aligned}
\tag{22}
$$

Hence, the fixed points of (20) are given by

$$
\begin{aligned}
&-\frac{\mu_1}{2}a_1+\left\{\frac{f_1}{2\omega_1}-\frac{\sigma_1 f_1}{4\omega_1^2}\right\}\sin\theta_1\\
&+\frac{\mu_1 f_1}{8\omega_1^2}\cos\theta_1-\frac{\alpha_1}{8\omega_1}a_1^2a_2\sin\theta_2\\
&-\frac{\alpha_2}{8\omega_1}a_1^2a_3\sin\theta_3-\frac{\alpha_4}{8\omega_1}a_2^2a_3\sin\left(\theta_3-2\theta_2\right)\\
&-\frac{\alpha_6}{4\omega_1}a_3^2a_2\sin\theta_2-\frac{3\alpha_8}{8\omega_1}a_2^3\sin\theta_2\\
&-\frac{\alpha_{10}}{8\omega_1}a_1a_2a_3\sin\left(\theta_3-\theta_2\right)=0,\\
&a_1\sigma_1+\left\{\frac{\mu_1^2}{8\omega_1}-\frac{\Gamma_1}{2\omega_1}\right\}a_1\\
&+\left\{\frac{f_1}{2\omega_1}-\frac{\sigma_1 f_1}{4\omega_1^2}\right\}\cos\theta_1-\frac{\mu_1 f_1}{8\omega_1^2}\sin\theta_1\\
&-\frac{3\alpha_1}{8\omega_1}a_1^2a_2\cos\theta_2-\frac{\alpha_2}{8\omega_1}a_1^2a_3\cos\theta_3\\
&-\frac{\alpha_3}{4\omega_1}a_1a_2^2-\frac{\alpha_4}{8\omega_1}a_2^2a_3\cos\left(\theta_3-2\theta_2\right)-\frac{\alpha_5}{4\omega_1}a_1a_3^2\\
&-\frac{\alpha_6}{4\omega_1}a_3^2a_2\cos\theta_2-\frac{3\alpha_7}{8\omega_1}a_1^3-\frac{3\alpha_8}{8\omega_1}a_2^3\cos\theta_2\\
&-\frac{\alpha_{10}}{8\omega_1}a_1a_2a_3\cos\left(\theta_3-\theta_2\right)=0,\\
&-\frac{\mu_2}{2}a_2+\left\{\frac{f_2}{2\omega_2}-\frac{\left(\sigma_1-\sigma_2\right)f_2}{4\omega_2^2}\right\}\sin\left(\theta_1-\theta_2\right)\\
&+\frac{\mu_2 f_2}{8\omega_2^2}\cos\left(\theta_1-\theta_2\right)\\
&+\frac{\beta_1}{8\omega_2}a_1^2a_2\sin 2\theta_2-\frac{\beta_2}{8\omega_2}a_1^2a_3\sin\left(\theta_3-\theta_2\right)
\end{aligned}
$$

$$+\frac{\beta_3}{8\omega_2}a_2^2a_1\sin\theta_2-\frac{\beta_4}{8\omega_2}a_2^2a_3\sin(\theta_3-3\theta_2)$$
$$+\frac{\beta_5}{4\omega_2}a_3^2a_1\sin\theta_2+\frac{3\beta_7}{8\omega_2}a_1^3\sin\theta_2$$
$$-\frac{\beta_{10}}{8\omega_2}a_1a_2a_3\sin(\theta_3-2\theta_2)=0,$$
$$a_2(\sigma_2-\sigma_1)-\left\{\frac{\mu_2^2}{8\omega_2}-\frac{\Gamma_2}{2\omega_2}\right\}a_2$$
$$+\left\{\frac{(\sigma_1-\sigma_2)f_2}{4\omega_2^2}-\frac{f_2}{2\omega_2}\right\}\cos(\theta_1-\theta_2)$$
$$+\frac{\mu_2f_2}{8\omega_2^2}\sin(\theta_1-\theta_2)+\frac{\beta_1}{8\omega_2}a_1^2a_2\cos 2\theta_2$$
$$+\frac{\beta_1}{4\omega_2}a_1^2a_2+\frac{\beta_2}{8\omega_2}a_1^2a_3\cos(\theta_3-\theta_2)$$
$$+\frac{3\beta_3}{8\omega_2}a_2^2a_1\cos\theta_2+\frac{\beta_4}{8\omega_2}a_2^2a_3\cos(\theta_3-3\theta_2)$$
$$+\frac{\beta_5}{4\omega_2}a_3^2a_1\cos\theta_2+\frac{\beta_6}{4\omega_2}a_3^2a_2+\frac{3\beta_7}{8\omega_2}a_1^3\cos\theta_2$$
$$+\frac{3\beta_8}{8\omega_2}a_2^3+\frac{\beta_{10}}{8\omega_2}a_1a_2a_3\cos(\theta_3-2\theta_2)=0,$$
$$-\frac{\mu_3}{2}a_3-\frac{\gamma_1}{8\omega_3}a_1^2a_2\sin(\theta_2-\theta_3)-\frac{\gamma_3}{8\omega_3}a_2^2a_1\sin(2\theta_2-\theta_3)$$
$$+\frac{\gamma_7}{8\omega_3}a_1^3\sin\theta_3-\frac{\gamma_8}{8\omega_3}a_2^3\sin(3\theta_2-\theta_3)=0,$$
$$a_3(\sigma_3-3\sigma_1)-\left\{\frac{\mu_3^2}{8\omega_3}-\frac{\Gamma_3}{2\omega_3}\right\}a_3+\frac{\gamma_1}{8\omega_3}a_1^2a_2\cos(\theta_2-\theta_3)$$
$$+\frac{\gamma_2}{4\omega_3}a_1^2a_3+\frac{\gamma_3}{8\omega_3}a_2^2a_1\cos(2\theta_2-\theta_3)$$
$$+\frac{\gamma_4}{4\omega_3}a_2^2a_3+\frac{\gamma_7}{8\omega_3}a_1^3\cos\theta_3+\frac{\gamma_8}{8\omega_3}a_2^3\cos(3\theta_2-\theta_3)$$
$$+\frac{3\gamma_9}{8\omega_3}a_3^3+\frac{\gamma_{10}}{4\omega_3}a_1a_2a_3\cos\theta_2=0. \tag{23}$$

There are six possibilities besides the trivial solution as follows:

(1) $a_1\neq 0, a_2=0, a_3=0$ (single mode),

(2) $a_2\neq 0, a_1=0, a_3=0$ (single mode),

(3) $a_1\neq 0, a_2\neq 0, a_3=0$ (two modes),

(4) $a_1\neq 0, a_3\neq 0, a_2=0$ (two modes),

(5) $a_2\neq 0, a_3\neq 0, a_1=0$ (two modes),

(6) $a_1\neq 0, a_2\neq 0, a_3\neq 0$ (three modes).

Case 1. In this case, where $a_2=0$, $a_3=0$, the frequency response equation is given by

$$\frac{9\alpha_7^2}{64\omega_1^2}a_1^6+\left[R_3+\frac{3\alpha_7\sigma_1}{4\omega_1}\right]a_1^4+\left[R_2+\sigma_1^2+\frac{\mu_1^2\sigma_1}{4\omega_1}-\frac{\Gamma_1\sigma_1}{\omega_1}\right]a_1^2$$
$$-\frac{\mu_1^2f_1^2}{64\omega_1^4}-R_1^2=0. \tag{24}$$

Case 2. In this case, where $a_1=0$, $a_3=0$, the frequency response equation is given by

$$\frac{9\beta_8^2}{64\omega_2^2}a_2^6+\left[Q_3+\frac{3\beta_8(\sigma_2-\sigma_1)}{4\omega_2}\right]a_2^4$$
$$+\left[Q_2+(\sigma_2-\sigma_1)^2-\frac{\mu_2^2(\sigma_2-\sigma_1)}{4\omega_2}+\frac{\Gamma_2(\sigma_2-\sigma_1)}{\omega_2}\right]a_2^2$$
$$-\frac{\mu_2^2f_2^2}{64\omega_2^4}-Q_1^2=0. \tag{25}$$

Case 3. In this case, where $a_3=0$, the frequency response equations are given by

$$\frac{9\alpha_7^2}{64\omega_1^2}a_1^6+\left[R_3+\frac{3\alpha_7\sigma_1}{4\omega_1}\right]a_1^4+\left[R_2+\sigma_1^2+\frac{\mu_1^2\sigma_1}{4\omega_1}-\frac{\Gamma_1\sigma_1}{\omega_1}\right]a_1^2$$
$$-\frac{\mu_1^2f_1^2}{64\omega_1^4}-R_1^2-\frac{9\alpha_1^2}{64\omega_1^2}a_1^4a_2^2-\frac{9\alpha_1\alpha_8}{32\omega_1^2}a_1^2a_2^4$$
$$-\frac{9\alpha_8^2}{64\omega_1^2}a_2^6+\frac{3R_1\alpha_8}{4\omega_1}a_2^3+\frac{3R_1\alpha_1}{4\omega_1}a_1^2a_2=0,$$
$$\frac{9\beta_8^2}{64\omega_2^2}a_2^6+\left[Q_3+\frac{3\beta_8(\sigma_2-\sigma_1)}{4\omega_2}\right]a_2^4$$
$$+\left[Q_2+(\sigma_2-\sigma_1)^2-\frac{\mu_2^2(\sigma_2-\sigma_1)}{4\omega_2}+\frac{\Gamma_2(\sigma_2-\sigma_1)}{\omega_2}\right]a_2^2$$
$$-\frac{\mu_2^2f_2^2}{64\omega_2^4}-Q_1^2+\frac{3Q_1\beta_3}{4\omega_2}a_2^2a_1+\frac{3Q_1\beta_7}{4\omega_2}a_1^3+\frac{Q_1\beta_1}{4\omega_2}a_1^2a_2$$
$$-\frac{9\beta_3^2}{64\omega_2^2}a_2^4a_1^2-\left[\frac{\beta_1^2}{64\omega_2^2}+\frac{9\beta_3\beta_7}{32\omega_2^2}\right]a_1^4a_2^2-\frac{9\beta_7^2}{64\omega_2^2}a_1^6$$
$$-\frac{3\beta_1\beta_7}{32\omega_2^2}a_1^5a_2-\frac{3\beta_1\beta_3}{32\omega_2^2}a_1^3a_2^3=0. \tag{26}$$

Case 4. In this case, where $a_2=0$, the frequency response equations are given by

$$\frac{9\alpha_7^2}{64\omega_1^2}a_1^6+\left[R_3+\frac{3\alpha_7\sigma_1}{4\omega_1}\right]a_1^4+\left[R_2+\sigma_1^2+\frac{\mu_1^2\sigma_1}{4\omega_1}-\frac{\Gamma_1\sigma_1}{\omega_1}\right]a_1^2$$
$$-\frac{\mu_1^2f_1^2}{64\omega_1^4}-R_1^2-\frac{\alpha_2^2}{64\omega_1^2}a_1^4a_3^2+\frac{R_1\alpha_2}{4\omega_1}a_1^2a_3=0,$$

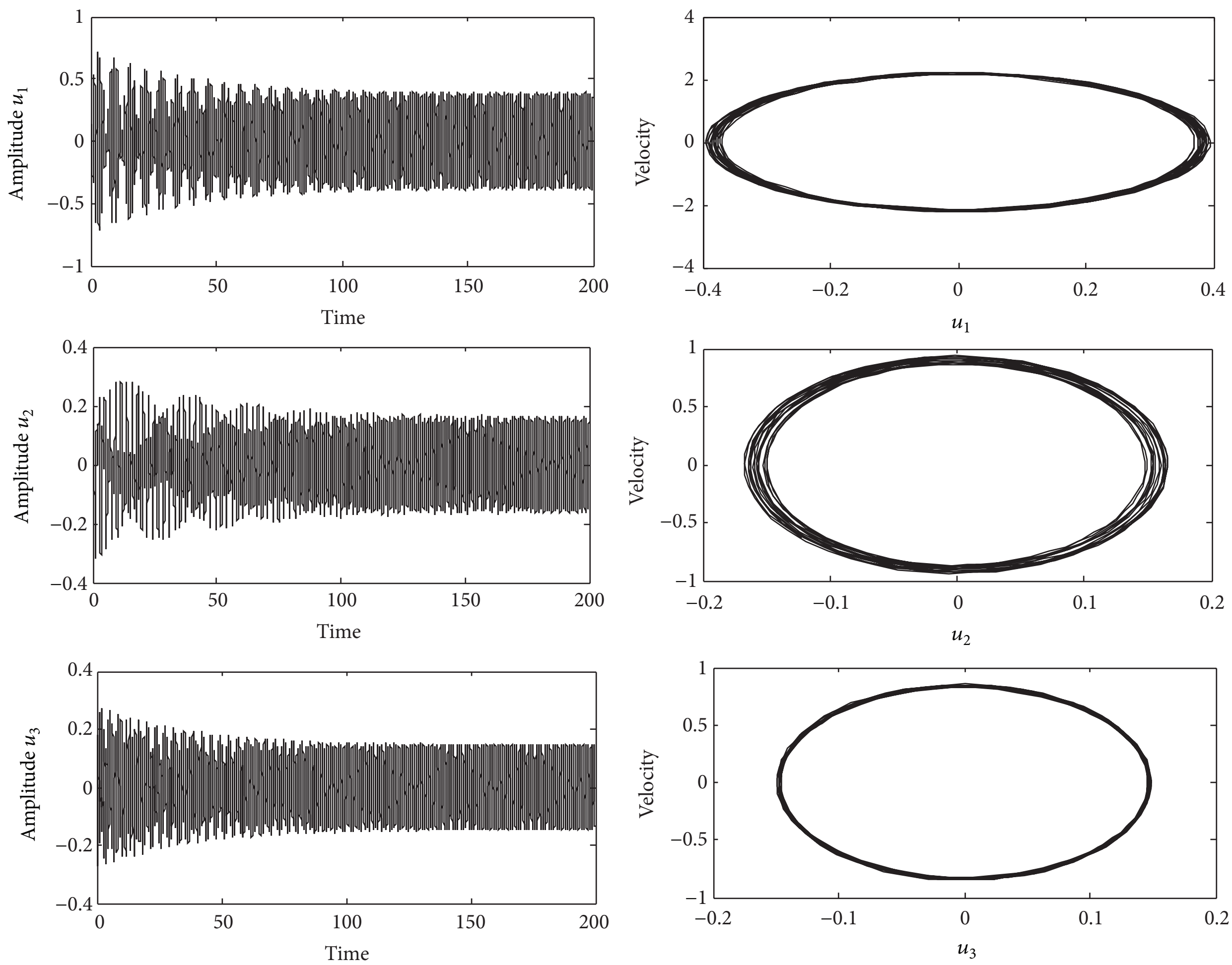

Figure 2: Time response and phase-plane diagrams of the system for nonresonance case.

$$\frac{9\gamma_9^2}{64\omega_3^2}a_3^6+\left[K_2+\frac{3\gamma_9(\sigma_3-3\sigma_1)}{4\omega_3}\right]a_3^4+\left[K_1+(\sigma_3-3\sigma_1)^2-\frac{\mu_3^2(\sigma_3-3\sigma_1)}{4\omega_3}+\frac{\Gamma_3(\sigma_3-3\sigma_1)}{\omega_3}\right]a_3^2-\frac{\gamma_7^2}{64\omega_3^2}a_1^6=0. \tag{27}$$

$$\frac{9\gamma_9^2}{64\omega_3^2}a_3^6+\left[K_2+\frac{3\gamma_9(\sigma_3-3\sigma_1)}{4\omega_3}\right]a_3^4+\left[K_1+(\sigma_3-3\sigma_1)^2-\frac{\mu_3^2(\sigma_3-3\sigma_1)}{4\omega_3}+\frac{\Gamma_3(\sigma_3-3\sigma_1)}{\omega_3}\right]a_3^2-\frac{\gamma_8^2}{64\omega_3^2}a_2^6=0. \tag{28}$$

Case 5. In this case, where $a_1 = 0$, the frequency response equations are given by

$$\frac{9\beta_8^2}{64\omega_2^2}a_2^6+\left[Q_3+\frac{3\beta_8(\sigma_2-\sigma_1)}{4\omega_2}\right]a_2^4+\left[Q_2+(\sigma_2-\sigma_1)^2-\frac{\mu_2^2(\sigma_2-\sigma_1)}{4\omega_2}+\frac{\Gamma_2(\sigma_2-\sigma_1)}{\omega_2}\right]a_2^2-\frac{\mu_2^2f_2^2}{64\omega_2^4}-Q_1^2+\frac{Q_1\beta_4}{4\omega_2}a_2^2a_3-\frac{\beta_4^2}{64\omega_2^2}a_2^4a_3^2=0,$$

Case 6. In this case, where $a_1\neq 0$, $a_2\neq 0$, and $a_3\neq 0$, this is the practical case, the frequency response equations are given by

$$\frac{9\alpha_7^2}{64\omega_1^2}a_1^6+\left[R_3+\frac{3\alpha_7\sigma_1}{4\omega_1}\right]a_1^4+\left[R_2+\sigma_1^2+\frac{\mu_1^2\sigma_1}{4\omega_1}-\frac{\Gamma_1\sigma_1}{\omega_1}\right]a_1^2-\frac{\mu_1^2f_1^2}{64\omega_1^4}-R_1^2+\frac{R_1\alpha_2}{4\omega_1}a_1^2a_3+\frac{R_1\alpha_6}{2\omega_1}a_2a_3^2+\frac{R_1\alpha_4}{4\omega_1}a_2^2a_3+\frac{3R_1\alpha_8}{4\omega_1}a_2^3+\frac{3R_1\alpha_1}{4\omega_1}a_1^2a_2+\frac{R_1\alpha_{10}}{4\omega_1}a_1a_2a_3-\frac{\alpha_6^2}{16\omega_1^2}a_2^2a_3^4$$

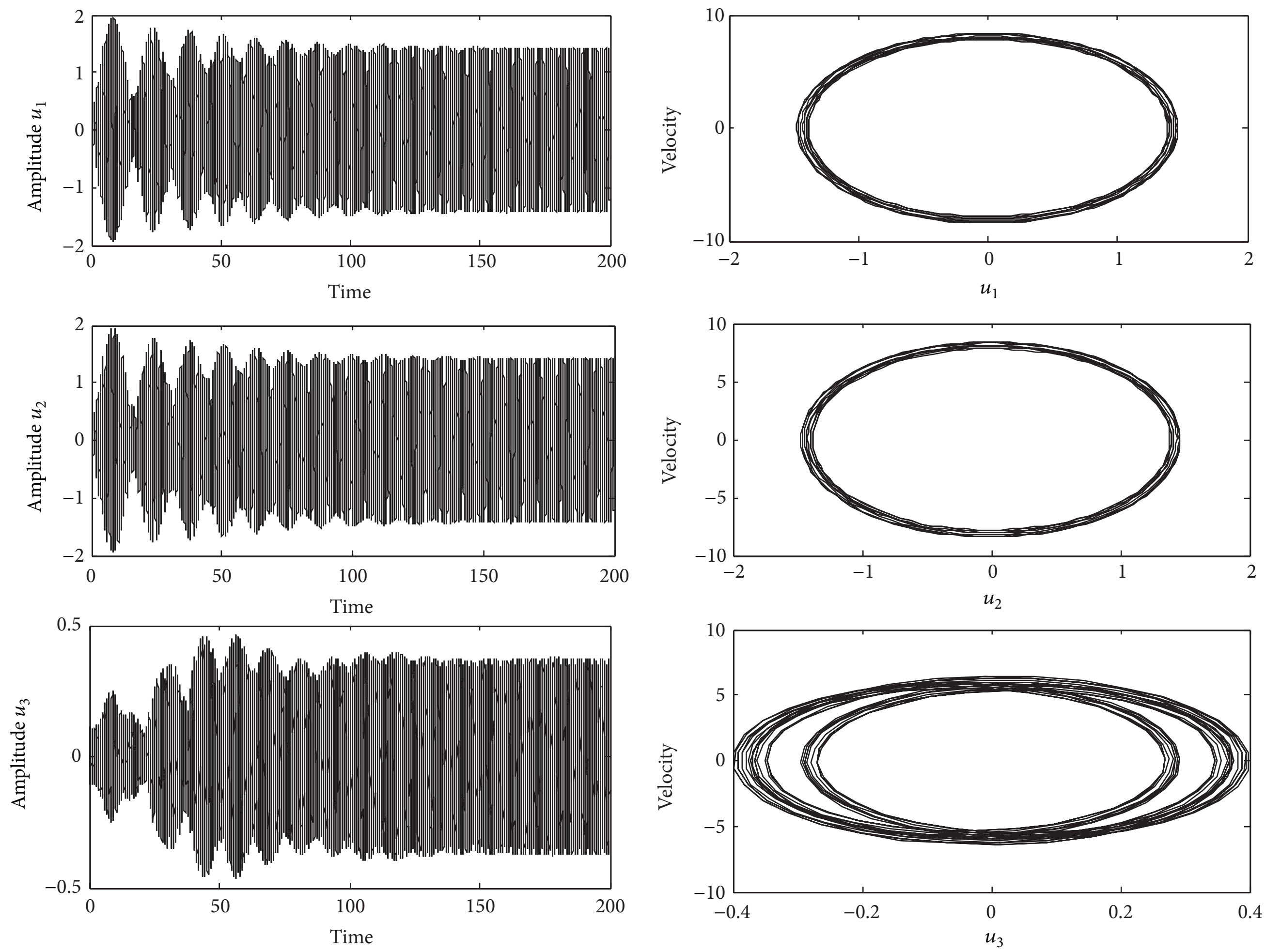

FIGURE 3: Time response and phase-plane diagrams of the system at simultaneous resonance case, $\Omega_3 \cong \omega_1$, $\omega_2 \cong \omega_1$, and $\omega_3 \cong 3\omega_1$.

$$- \frac{\alpha_4\alpha_6}{16\omega_1^2} a_2^3 a_3^3 - \frac{\alpha_2^2}{64\omega_1^2} a_1^4 a_3^2 - \frac{9\alpha_1^2}{64\omega_1^2} a_1^4 a_2^2 - \frac{9\alpha_1\alpha_8}{32\omega_1^2} a_1^2 a_2^4$$

$$- \frac{9\alpha_8^2}{64\omega_1^2} a_2^6 - \frac{3\alpha_4\alpha_8}{32\omega_1^2} a_2^5 a_3 - \frac{3\alpha_8\alpha_{10}}{32\omega_1^2} a_1 a_2^4 a_3 - \frac{\alpha_2\alpha_{10}}{32\omega_1^2} a_1^3 a_2 a_3^2$$

$$- \frac{\alpha_4\alpha_{10}}{32\omega_1^2} a_1 a_2^3 a_3^2 - \frac{\alpha_6\alpha_{10}}{16\omega_1^2} a_1 a_2^2 a_3^3 - \frac{\alpha_2\alpha_6}{16\omega_1^2} a_1^2 a_2 a_3^3$$

$$- \frac{3\alpha_1\alpha_{10}}{32\omega_1^2} a_1^3 a_2^2 a_3 - \frac{3\alpha_1\alpha_2}{32\omega_1^2} a_1^4 a_2 a_3 - R_4 a_1^2 a_2^2 a_3^2$$

$$- R_5 a_2^4 a_3^2 - R_6 a_2^3 a_1^2 a_3 = 0,$$

$$\frac{9\beta_8^2}{64\omega_2^2} a_2^6 + \left[Q_3 + \frac{3\beta_8 (\sigma_2 - \sigma_1)}{4\omega_2} \right] a_2^4$$

$$+ \left[Q_2 + (\sigma_2 - \sigma_1)^2 - \frac{\mu_2^2 (\sigma_2 - \sigma_1)}{4\omega_2} + \frac{\Gamma_2 (\sigma_2 - \sigma_1)}{\omega_2} \right] a_2^2$$

$$- \frac{\mu_2^2 f_2^2}{64\omega_2^4} - Q_1^2 + \frac{3Q_1\beta_3}{4\omega_2} a_2^2 a_1 + \frac{3Q_1\beta_7}{4\omega_2} a_1^3 + \frac{Q_1\beta_1}{4\omega_2} a_1^2 a_2$$

$$+ \frac{Q_1\beta_4}{4\omega_2} a_2^2 a_3 + \frac{Q_1\beta_5}{2\omega_2} a_1 a_3^2 + \frac{Q_1\beta_2}{4\omega_2} a_1^2 a_3 + \frac{Q_1\beta_{10}}{4\omega_2} a_1 a_2 a_3$$

$$- \frac{3\beta_1\beta_7}{32\omega_2^2} a_1^5 a_2 - \frac{9\beta_3^2}{64\omega_2^2} a_2^4 a_1^2 - \frac{9\beta_7^2}{64\omega_2^2} a_1^6 - \frac{\beta_4^2}{64\omega_2^2} a_2^4 a_3^2$$

$$- \frac{3\beta_1\beta_3}{32\omega_2^2} a_1^3 a_2^3 - \frac{\beta_5^2}{16\omega_2^2} a_1^2 a_3^4 - \frac{\beta_2\beta_5}{16\omega_2^2} a_1^3 a_3^3 - \frac{3\beta_3\beta_4}{32\omega_2^2} a_1 a_2^4 a_3$$

$$- \frac{3\beta_2\beta_7}{32\omega_2^2} a_1^5 a_3 - \frac{\beta_4\beta_5}{16\omega_2^2} a_1 a_2^2 a_3^3 - \frac{\beta_5\beta_{10}}{16\omega_2^2} a_1^2 a_2 a_2^3 - \frac{\beta_4\beta_{10}}{32\omega_2^2} a_1 a_2^3 a_3^2$$

$$- Q_4 a_1^2 a_2^2 a_3^2 - Q_5 a_1^4 a_2^2 - Q_6 a_1^4 a_3^2 - Q_7 a_1^3 a_2^2 a_3 - Q_8 a_1^2 a_2^3 a_3$$

$$- Q_9 a_1^3 a_2 a_3^2 - Q_{10} a_1^4 a_2 a_3 = 0,$$

$$\frac{9\gamma_9^2}{64\omega_3^2} a_3^6 + \left[K_2 + \frac{3\gamma_9 (\sigma_3 - 3\sigma_1)}{4\omega_3} \right] a_3^4$$

$$+ \left[K_1 + (\sigma_3 - 3\sigma_1)^2 - \frac{\mu_3^2 (\sigma_3 - 3\sigma_1)}{4\omega_3} + \frac{\Gamma_3 (\sigma_3 - 3\sigma_1)}{\omega_3} \right] a_3^2$$

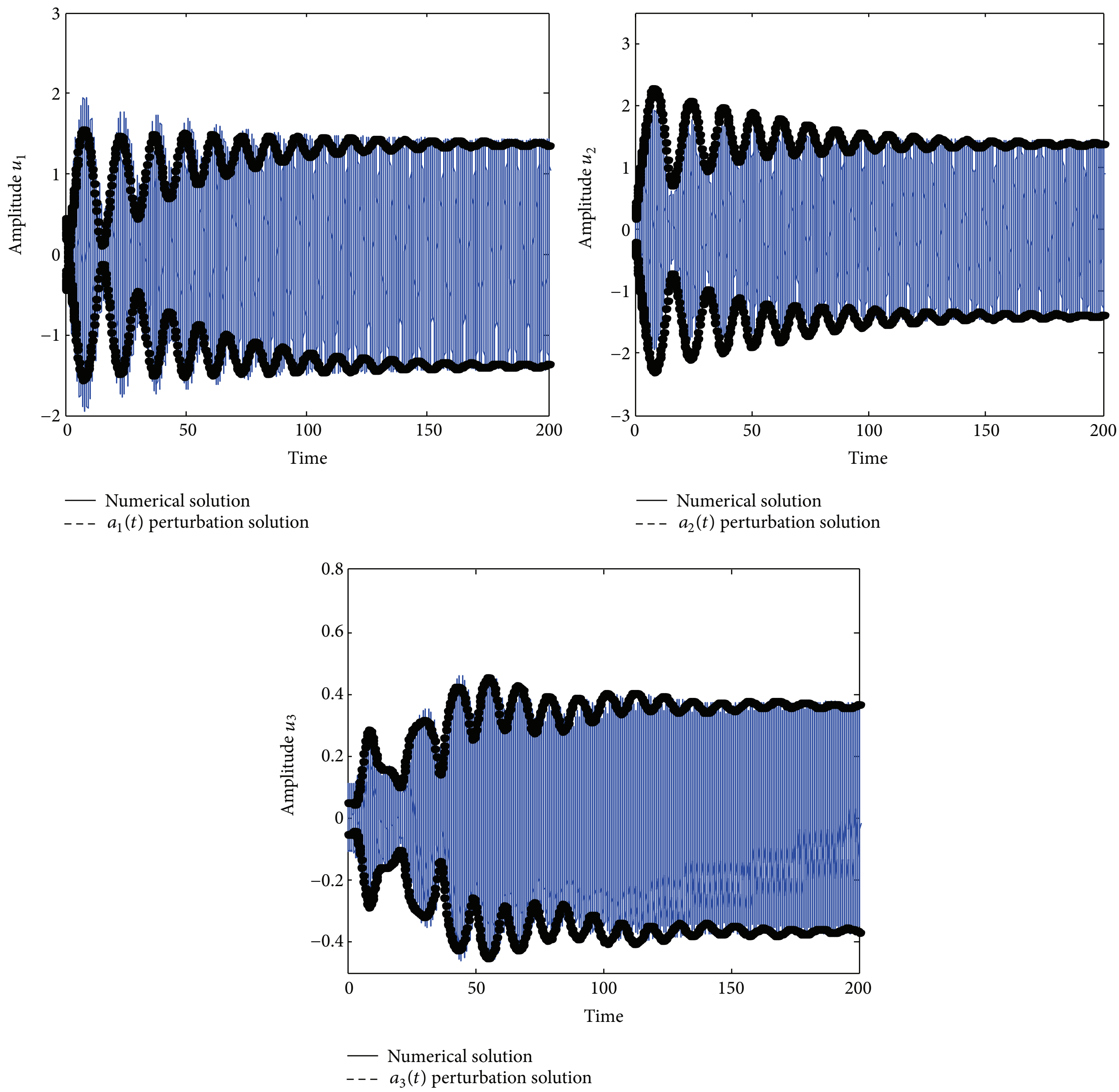

Figure 4: Comparison between numerical solution (using RKM) and analytical solution (using perturbation method) of the system at resonance case, $\Omega_3 \cong \omega_1$, $\omega_2 \cong \omega_1$, and $\omega_3 \cong 3\omega_1$.

$$-\frac{\gamma_8^2}{64\omega_3^2}a_2^6 - \frac{\gamma_7^2}{64\omega_3^2}a_1^6 - \frac{\gamma_1\gamma_7}{32\omega_3^2}a_1^5 a_2 - \frac{\gamma_3\gamma_8}{32\omega_3^2}a_1 a_2^5 - K_3 a_1^4 a_2^2 - K_4 a_1^2 a_2^4 - K_5 a_1^3 a_2^2 = 0, \tag{29}$$

where

$$R_1 = \left[\frac{f_1}{2\omega_1} - \frac{\sigma_1 f_1}{4\omega_1^2}\right],$$

$$R_2 = \left[\frac{\mu_1^2}{4} + \frac{\mu_1^4}{64\omega_1^2} + \frac{\Gamma_1^2}{4\omega_1^2} - \frac{\Gamma_1\mu_1^2}{8\omega_1^2}\right],$$

$$R_3 = \left[\frac{3\alpha_7\mu_1^2}{32\omega_1^2} - \frac{3\alpha_7\Gamma_1}{8\omega_1^2}\right],$$

$$R_4 = \left[\frac{\alpha_{10}^2}{64\omega_1^2} + \frac{3\alpha_1\alpha_6}{16\omega_1^2} + \frac{\alpha_2\alpha_4}{32\omega_1^2}\right],$$

$$R_5 = \left[\frac{3\alpha_6\alpha_8}{16\omega_1^2} + \frac{\alpha_4^2}{64\omega_1^2}\right],$$

$$R_6 = \left[\frac{3\alpha_1\alpha_4}{32\omega_1^2} + \frac{3\alpha_2\alpha_8}{32\omega_1^2}\right],$$

$$Q_1 = \left[\frac{f_2}{2\omega_2} - \frac{(\sigma_1 - \sigma_2)\ f_2}{4\omega_2^2}\right],$$

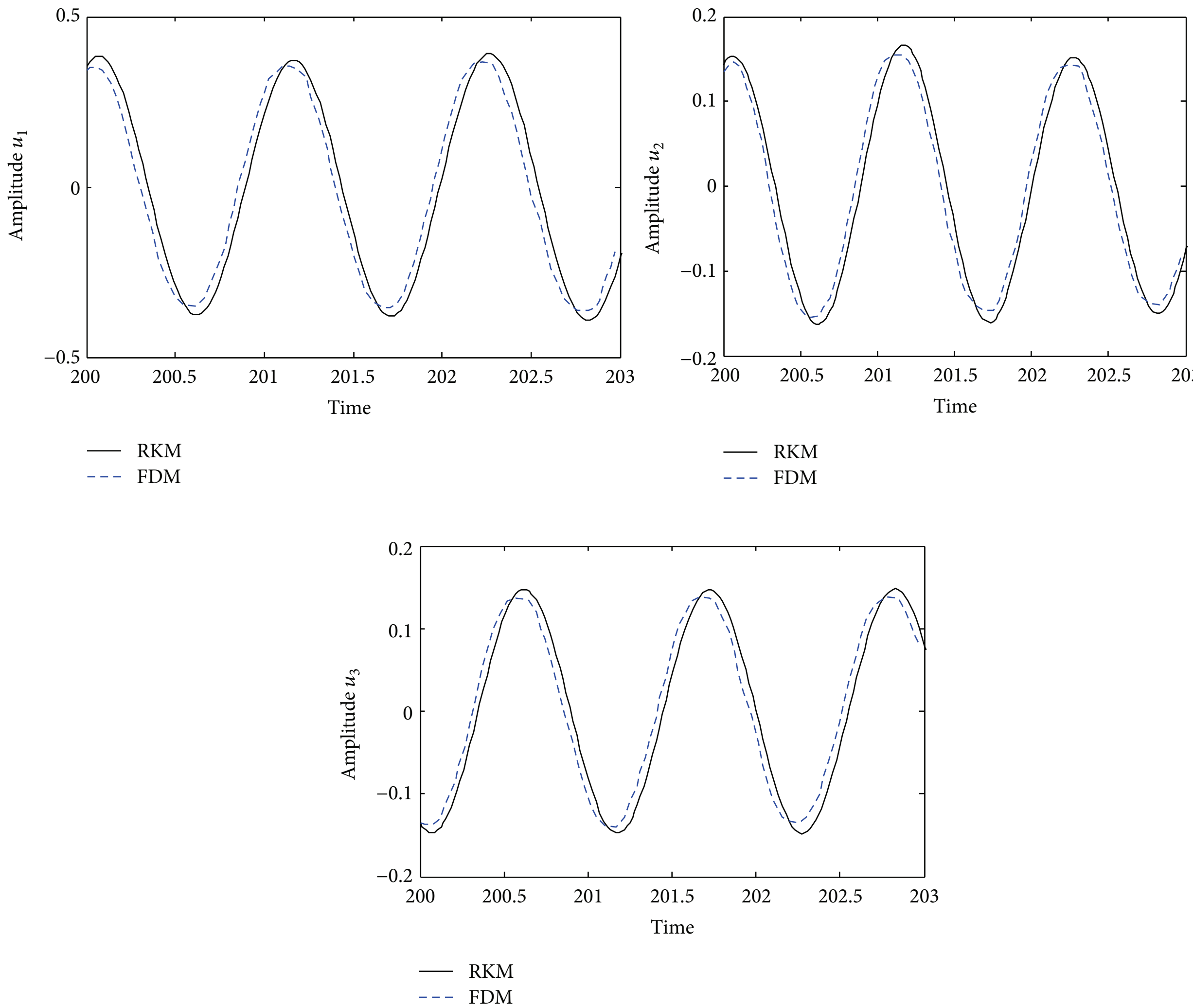

Figure 5: Time response of composite laminated rectangular plate using RKM and FDM.

$$
\begin{aligned}
Q_2 &= \left[\frac{\mu_2^2}{4} + \frac{\mu_2^4}{64\omega_2^2} + \frac{\Gamma_2^2}{4\omega_2^2} - \frac{\Gamma_2\mu_2^2}{8\omega_2^2}\right], \\
Q_3 &= \left[\frac{3\beta_8\Gamma_2}{8\omega_2^2} - \frac{3\beta_8\mu_2^2}{32\omega_2^2}\right], \\
Q_4 &= \left[\frac{\beta_{10}^2}{64\omega_2^2} + \frac{3\beta_3\beta_5}{16\omega_2^2} + \frac{\beta_2\beta_4}{32\omega_2^2}\right], \\
Q_5 &= \left[\frac{\beta_1^2}{64\omega_2^2} + \frac{9\beta_3\beta_7}{32\omega_2^2}\right], \\
Q_6 &= \left[\frac{\beta_2^2}{64\omega_2^2} + \frac{3\beta_5\beta_7}{16\omega_2^2}\right], \\
Q_7 &= \left[\frac{3\beta_2\beta_3}{32\omega_2^2} + \frac{3\beta_4\beta_7}{32\omega_2^2} + \frac{\beta_1\beta_{10}}{32\omega_2^2}\right], \\
Q_8 &= \left[\frac{3\beta_3\beta_{10}}{32\omega_2^2} + \frac{\beta_1\beta_4}{32\omega_2^2}\right], \\
Q_9 &= \left[\frac{\beta_2\beta_{10}}{32\omega_2^2} + \frac{\beta_1\beta_5}{16\omega_2^2}\right], \\
Q_{10} &= \left[\frac{3\beta_7\beta_{10}}{32\omega_2^2} + \frac{\beta_1\beta_2}{32\omega_2^2}\right], \\
K_1 &= \left[\frac{\mu_3^2}{4} + \frac{\mu_3^4}{64\omega_3^2} + \frac{\Gamma_3^2}{4\omega_3^2} - \frac{\Gamma_3\mu_3^2}{8\omega_3^2}\right], \\
K_2 &= \left[\frac{3\gamma_9\Gamma_3}{8\omega_3^2} - \frac{3\gamma_9\mu_3^2}{32\omega_3^2}\right], \\
K_3 &= \left[\frac{\gamma_1^2}{64\omega_3^2} + \frac{\gamma_3\gamma_7}{32\omega_3^2}\right], \\
K_4 &= \left[\frac{\gamma_3^2}{64\omega_3^2} + \frac{\gamma_1\gamma_8}{32\omega_3^2}\right], \\
K_5 &= \left[\frac{\gamma_1\gamma_3}{32\omega_3^2} + \frac{\gamma_7\gamma_8}{32\omega_3^2}\right].
\end{aligned}
\tag{30}
$$

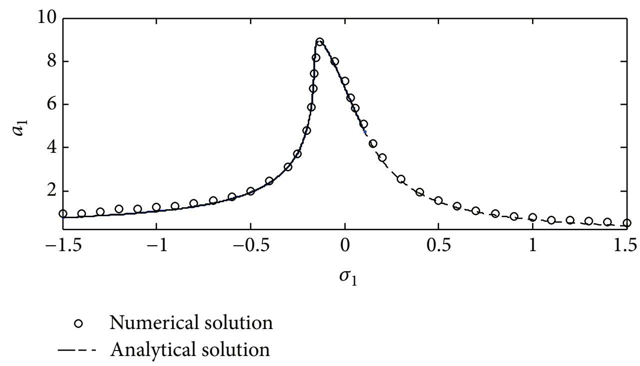

Figure 6: Comparison between analytical prediction using multiple time scale and numerical integration of the first mode.

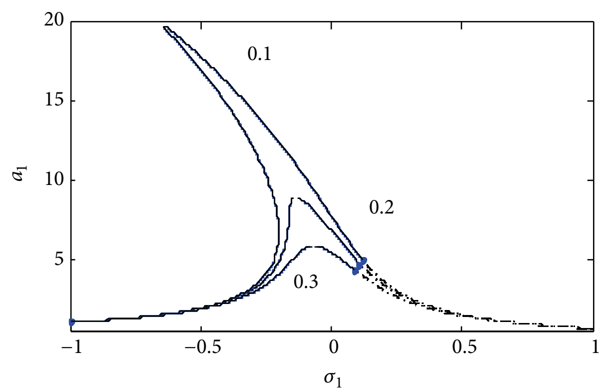

Figure 7: Effects of the linear damping μ_1.

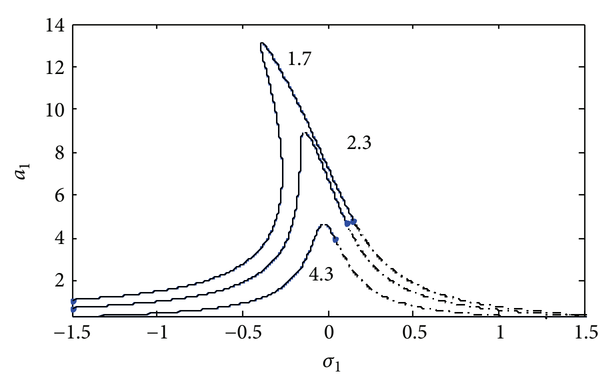

Figure 8: Effects of the natural frequency ω_1.

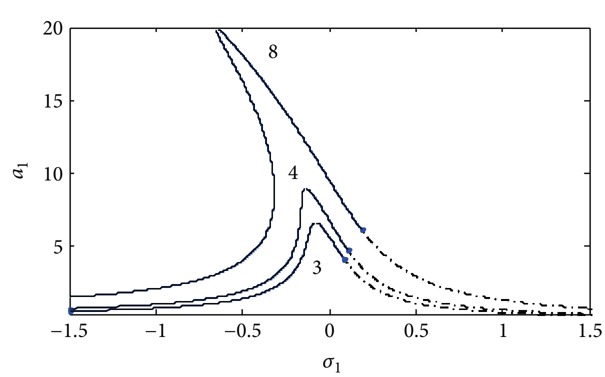

Figure 9: Effects of the external excitation f_1.

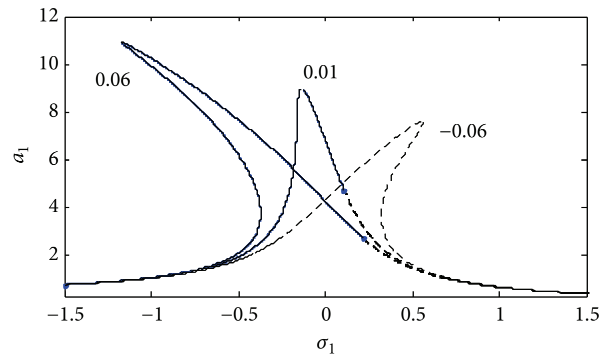

Figure 10: Effects of the nonlinear parameter α_7.

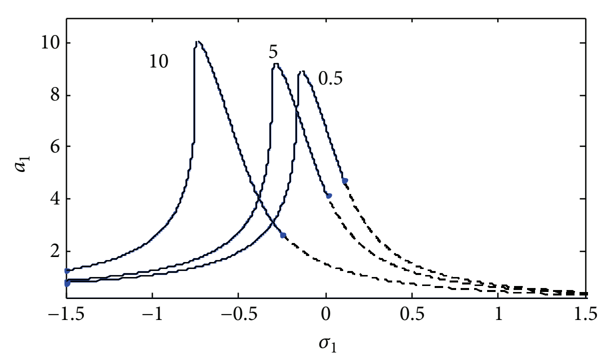

Figure 11: Effects of the parametric excitation f_{14}.

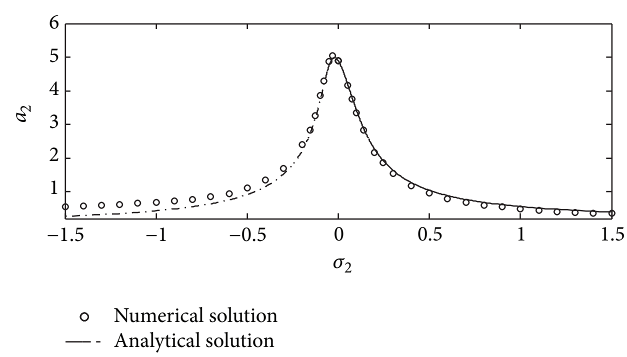

Figure 12: Comparison between analytical prediction using multiple time scale and numerical integration of the second mode.

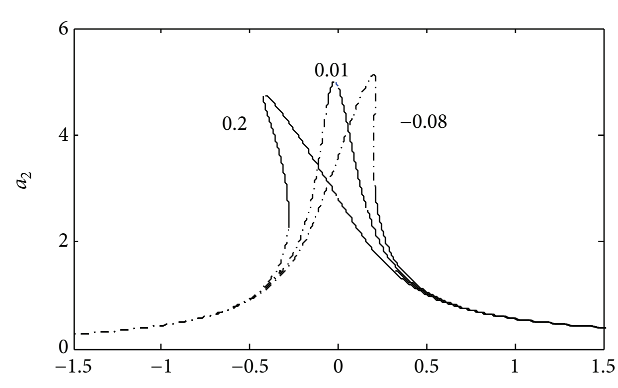

Figure 13: Effects of the nonlinear parameter β_8.

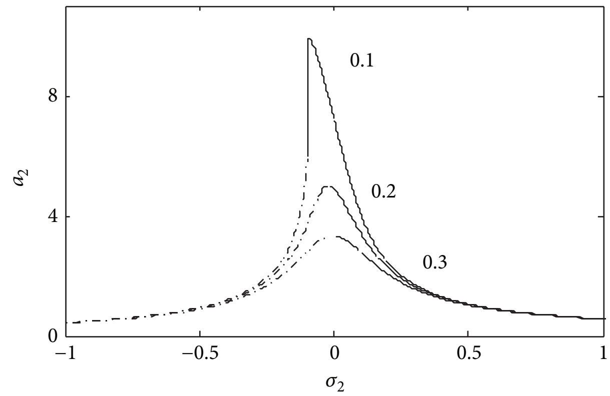

Figure 14: Effects of the linear damping μ_2.

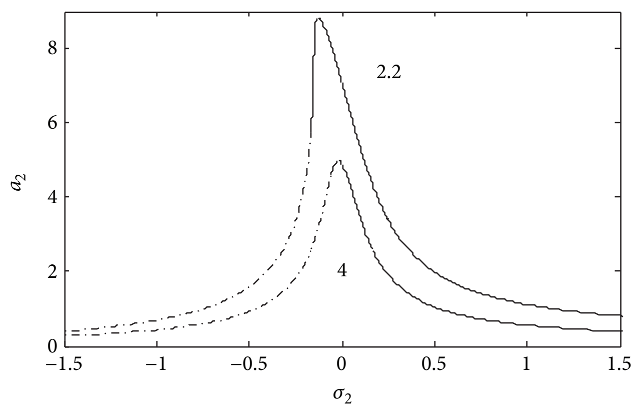

Figure 15: Effects of the natural frequency ω_2.

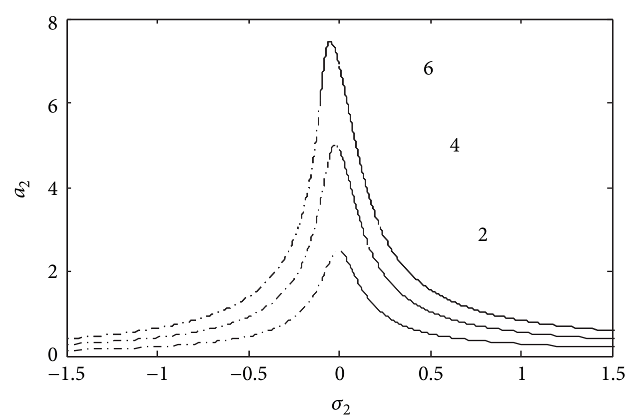

Figure 16: Effects of the external excitation f_2.

In the frequency response curves, the stable (unstable) steady-state solutions have been represented by solid (dotted) lines.

4. Numerical Results and Discussion

To study the behavior of the system, the Runge-Kutta fourth-order method (RKM) was applied to (4a), (4b), and (4c) governing the oscillating system. A good criterion of both stability and dynamic chaos is the phase plane trajectories. Figure 2 illustrates the response and the phase-plane for the nonresonant system at some practical values of the equation parameters: $\mu_1 = 0.05$, $\mu_2 = 0.05$, $\mu_3 = 0.05$, $\alpha_1 = \beta_1 = \gamma_1 = 1.5$, $\alpha_2 = \beta_2 = \gamma_2 = 1.9$, $\alpha_3 = \beta_3 = \gamma_3 = 0.4$, $\alpha_4 = \beta_4 = \gamma_4 = 0.6$, $\alpha_5 = \beta_5 = \gamma_5 = 0.6$, $\alpha_6 = \beta_6 = \gamma_6 = 0.2$, $\alpha_7 = \beta_7 = \gamma_7 = 0.01$, $\alpha_8 = \beta_8 = \gamma_8 = 0.01$, $\alpha_9 = \beta_9 = \gamma_9 = 0.4$, $\alpha_{10} = \beta_{10} = \gamma_{10} = 1.8$, $\Omega_1 = 6.4$, $\Omega_2 = 6.1$, $\Omega_3 = 5.7$, $\Omega_4 = 2$, $\omega_1 = 4.7$,

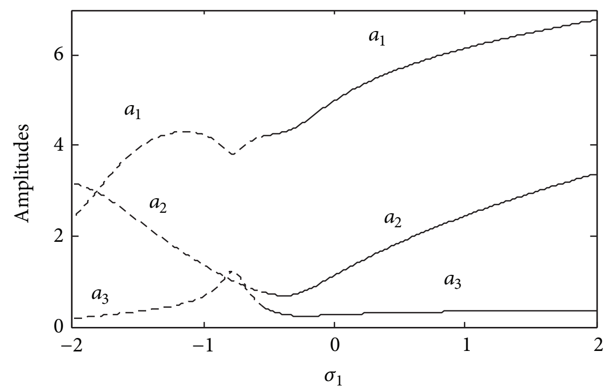

Figure 17: Effects of the detuning parameter σ_1.

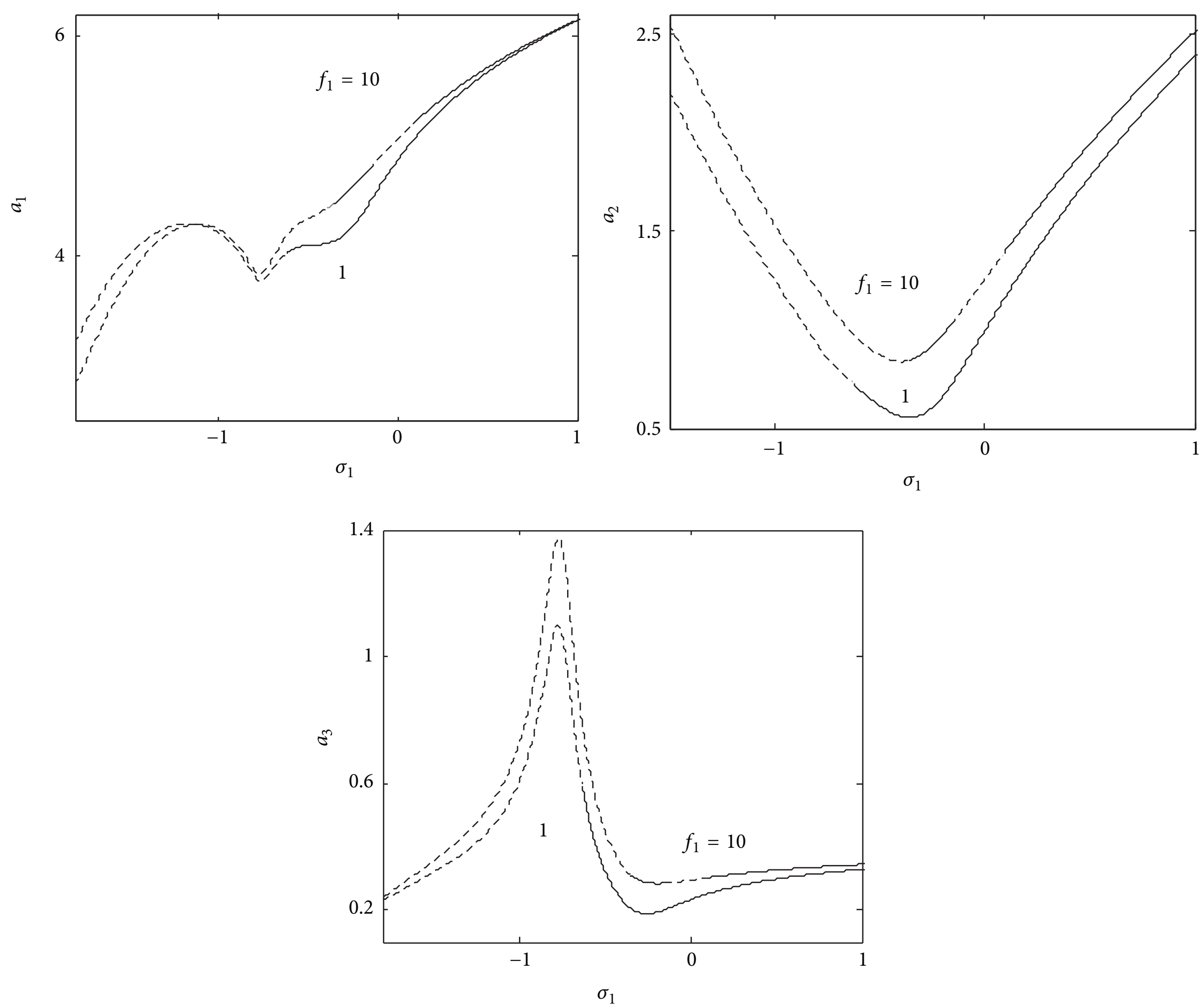

Figure 18: Effects of the external excitation force f_1.

$\omega_2 = 2.7$, $\omega_3 = 13.1$, $f_1 = f_2 = 4$, $f_3 = 20.5$, $f_{11} = f_{21} = f_{31} = 0.1$, $f_{12} = f_{22} = f_{32} = 0.2$, and $f_{14} = f_{24} = f_{34} = 0.5$. Figure 3 shows the steady-state amplitudes and phase plane of the system at simultaneous resonance case $\Omega_3 \cong \omega_1$, $\omega_2 \cong \omega_1$, and $\omega_3 \cong 3\omega_1$. It is clear from Figure 3 that the steady-state amplitude of the first, second, and third modes is increased to about 370%, 890%, and 260%, respectively, of its value shown in Figure 2. Also, it can be seen that the time response of the system is tuned with multilimit cycle.

It is quite clear that such case is undesirable in the design of such system because it represents one of the worst behaviors of the system. Such case should be avoided as

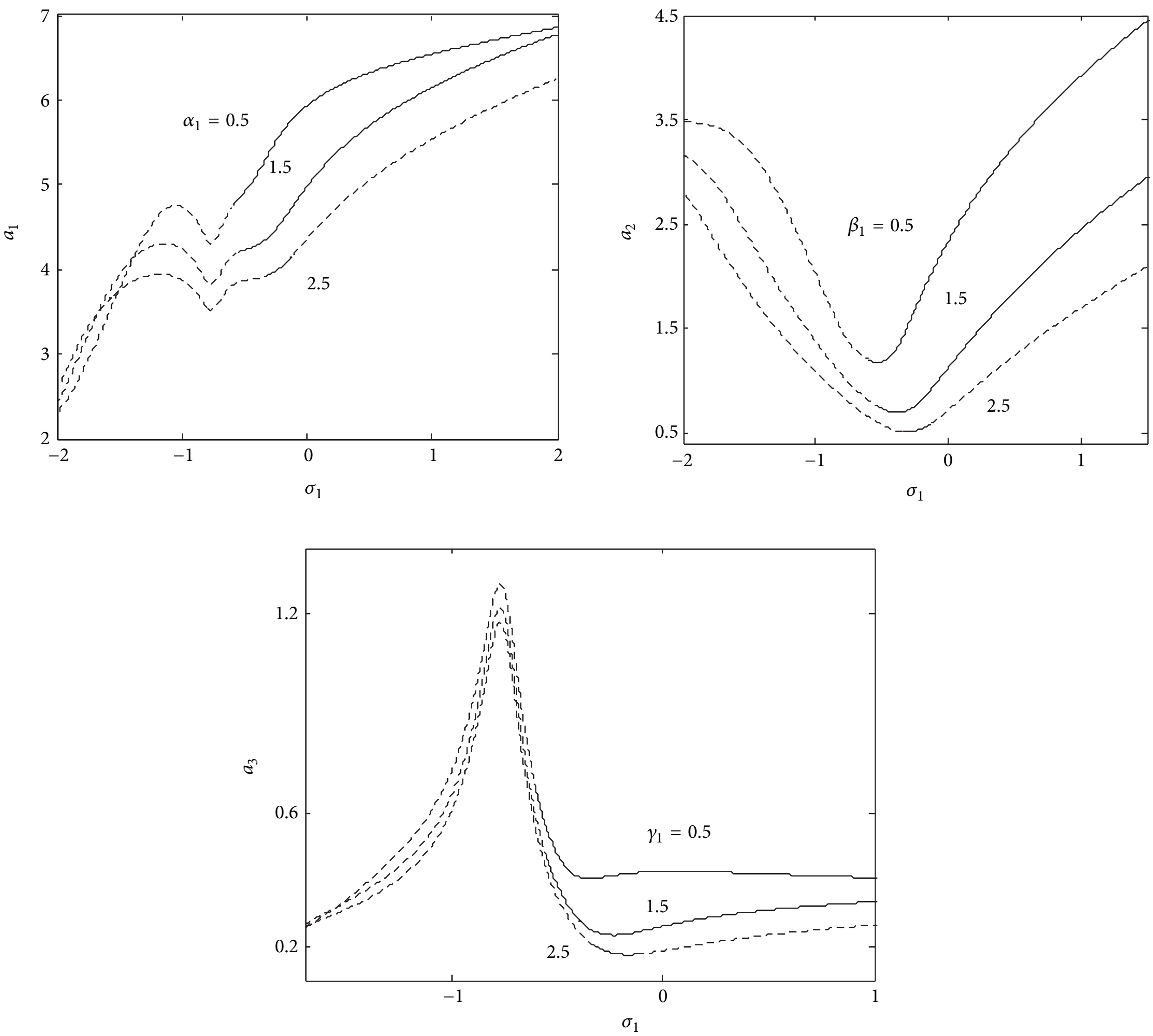

FIGURE 19: Effects of the nonlinear parameters (α_1, β_1, and γ_1 coupling terms).

working condition for the system. It is advised for such system not to have $\omega_2 = \omega_1$ or $\omega_3 = 3\omega_1$. Figure 4 shows the comparison between numerical integration for the system equation (4a), (4b), and (4c) solid lines and the amplitude-phase modulating equation (20) dashed lines. We found that all predictions from analytical solutions dashed lines are in good agreement with the numerical simulation solid lines.

4.1. FDM with Approximation O(c^2). The infinite equations (2a)–(2e) will be solved via a finite difference method (FDM). We briefly describe the procedure here. More details are available in [23, 26]. The infinite dimensional equations (2a)–(2e) can be reduced to the finite dimensional one via the finite difference method with second-order approximation $O(c^2)$. Namely, at each mesh node the following system of ordinary differential equations is obtained:

$$\begin{aligned}
L_{1,c}\left(N_{xx}, N_{xy}\right) &= I_0(\ddot{u}_0)_{i,j} + J_1\left(\ddot{\phi}_x\right)_{i,j} \\
&\quad - \frac{2}{3h^2c} I_3\left((\ddot{w}_0)_{i+1,j} - (\ddot{w}_0)_{i-1,j}\right), \\
L_{2,c}\left(N_{xy}, N_{yy}\right) &= I_0(\ddot{v}_0)_{i,j} + J_1\left(\ddot{\phi}_y\right)_{i,j} \\
&\quad - \frac{2}{3h^2c} I_3\left((\ddot{w}_0)_{i,j+1} - (\ddot{w}_0)_{i,j-1}\right), \\
&L_{3,c}\left(\overline{Q}_x, \overline{Q}_y, N_{xx}, w_0, N_{xy}\right) \\
&= I_0(\ddot{w}_0)_{i,j} - \frac{16}{9h^4c^2} I_6\left((\ddot{w}_0)_{i+1,j} - 2(\ddot{w}_0)_{i,j} + (\ddot{w}_0)_{i+1,j}\right. \\
&\quad \left. + (\ddot{w}_0)_{i,j+1} - 2(\ddot{w}_0)_{i,j} + (\ddot{w}_0)_{i,j+1}\right)
\end{aligned}$$

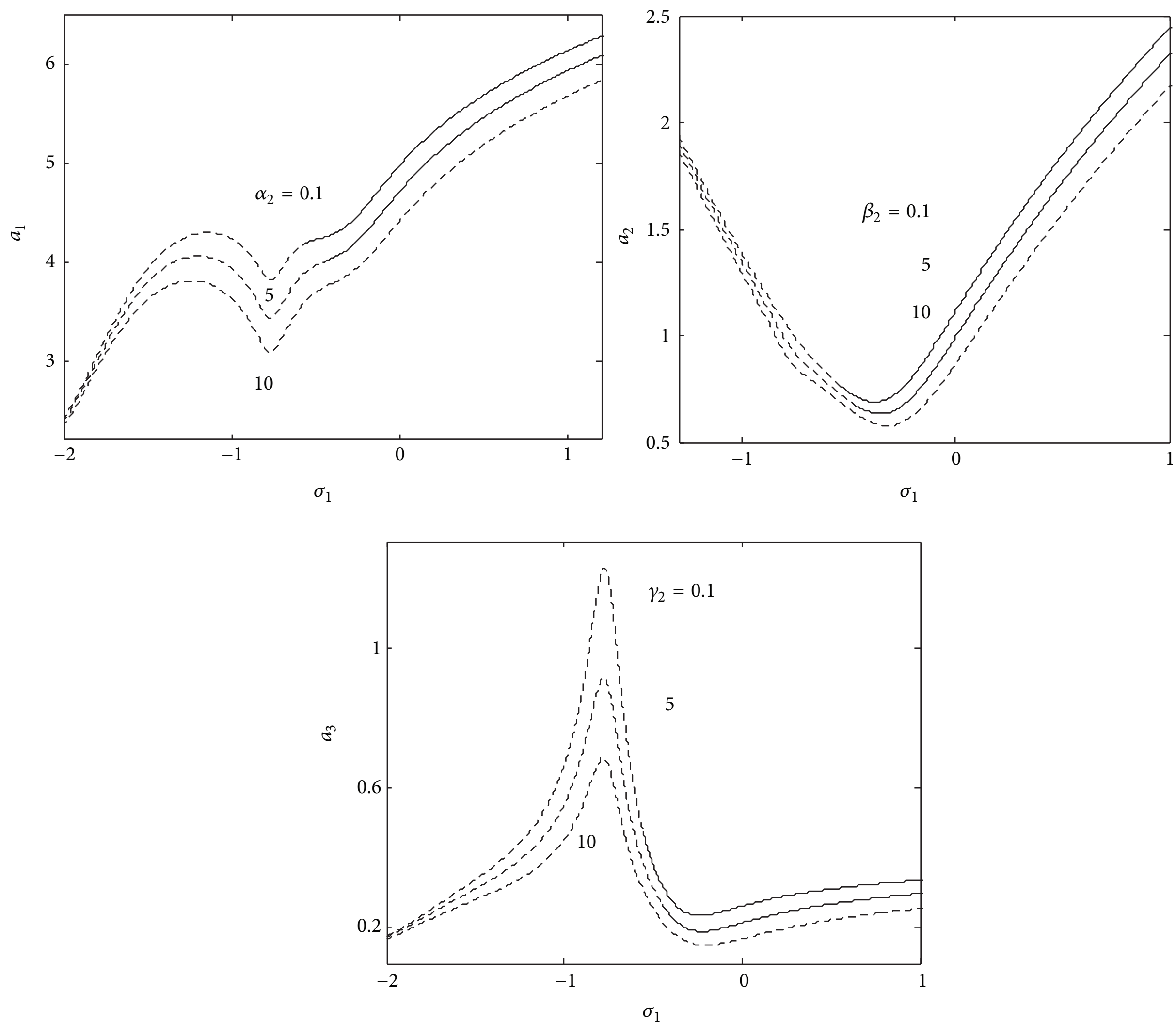

Figure 20: Effects of the nonlinear parameters (α_2, β_2, and γ_2 coupling terms).

$$
\begin{aligned}
&+\frac{4}{3h^2c^2}I_3\left(\left(\ddot{u}_0\right)_{i+1,j}-\left(\ddot{u}_0\right)_{i-1,j}+\left(\ddot{v}_0\right)_{i,j+1}-\left(\ddot{v}_0\right)_{i,j-1}\right)\\
&+\frac{J_4}{2c}\left(\left(\ddot{\phi}_x\right)_{i+1,j}-\left(\ddot{\phi}_x\right)_{i-1,j}+\left(\ddot{\phi}_y\right)_{i,j+1}-\left(\ddot{\phi}_y\right)_{i,j-1}\right),\\
L_{4,c}&\left(\overline{M}_{xx},\overline{M}_{xy}\right)=J_1\left(\ddot{u}_0\right)_{i,j}+k_2\left(\ddot{\phi}_x\right)_{i,j}\\
&-\frac{2J_4}{3h^2c}\left(\left(\ddot{w}_0\right)_{i+1,j}-\left(\ddot{w}_0\right)_{i-1,j}\right),\\
L_{5,c}&\left(\overline{M}_{xy},\overline{M}_{yy}\right)=J_1\left(\ddot{v}_0\right)_{i,j}+k_2\left(\ddot{\phi}_y\right)_{i,j}\\
&-\frac{2J_4}{3h^2c}\left(\left(\ddot{w}_0\right)_{i,j+1}-\left(\ddot{w}_0\right)_{i,j-1}\right),\\
&(i=1,2,\ldots,n),\ (j=1,2,\ldots,n),
\end{aligned}
\tag{31}
$$

where n denotes the partition number regarding a spatial coordinate, c is the computational step regarding spatial coordinate, and $L_{1,c}(\cdot)$, $L_{2,c}(\cdot)$, $L_{3,c}(\cdot)$, $L_{4,c}(\cdot)$, and $L_{5,c}(\cdot)$ are the difference operators as follows:

$$
\begin{aligned}
L_{1,c}\left(N_{xx},N_{xy}\right)&=\frac{1}{2c}\left(\left(N_{xx}\right)_{i+1,j}-\left(N_{xx}\right)_{i-1,j}+\left(N_{xy}\right)_{i,j+1}-\left(N_{xy}\right)_{i,j-1}\right),\\
L_{2,c}\left(N_{xy},N_{yy}\right)&=\frac{1}{2c}\left(\left(N_{xy}\right)_{i+1,j}-\left(N_{xy}\right)_{i-1,j}+\left(N_{yy}\right)_{i,j+1}-\left(N_{yy}\right)_{i,j-1}\right),
\end{aligned}
$$

$$L_{3,c}\left(\overline{Q}_x,\overline{Q}_y,N_{xx},w_0,N_{xy}\right)=\frac{1}{2c}\left(\left(\overline{Q}_x\right)_{i+1,j}-\left(\overline{Q}_x\right)_{i-1,j}+\left(\overline{Q}_y\right)_{i,j+1}-\left(\overline{Q}_y\right)_{i,j-1}\right)$$
$$+N_{xx}\left(\frac{(w_0)_{i-1,j}-2(w_0)_{i,j}+(w_0)_{i+1,j}}{c^2}\right)+\left(\frac{(w_0)_{i+1,j}-(w_0)_{i-1,j}}{2c}\right)\left(\frac{(N_{xx})_{i+1,j}-(N_{xx})_{i-1,j}}{2c}\right)$$
$$+N_{xy}\left(\frac{\left((w_0)_{j+1,i+1}-2(w_0)_{j+1,i-1}\right)\left((w_0)_{j-1,i+1}-2(w_0)_{j-1,i-1}\right)}{4c^2}\right)$$
$$+\left(\frac{(w_0)_{i,j+1}-(w_0)_{i,j-1}}{2c}\right)\left(\frac{\left(N_{xy}\right)_{i+1,j}-\left(N_{xy}\right)_{i-1,j}}{2c}\right)$$
$$+N_{xy}\left(\frac{\left((w_0)_{i+1,j+1}-(w_0)_{i+1,j-1}\right)-\left((w_0)_{i-1,j+1}-(w_0)_{i-1,j-1}\right)}{8c^3}\right)$$
$$+\left(\frac{(w_0)_{i+1,j}-(w_0)_{i-1,j}}{2c}\right)\left(\frac{\left(N_{yy}\right)_{i,j+1}-\left(N_{yy}\right)_{i,j-1}}{2c}\right)+N_{yy}\left(\frac{(w_0)_{i,j-1}-2(w_0)_{i,j}+(w_0)_{i,j+1}}{c^2}\right)$$
$$+\left(\frac{(w_0)_{i,j+1}-(w_0)_{i,j-1}}{2c}\right)\left(\frac{\left(N_{yy}\right)_{i,j+1}-\left(N_{yy}\right)_{i,j-1}}{2c}\right)+\frac{4}{3h^2}\left(\frac{(P_{xx})_{i-1,j}-2(P_{xx})_{i,j}+(P_{xx})_{i+1,j}}{c^2}\right)$$
$$+\frac{4}{3h^2}\left(2\left(\frac{\left(\left(P_{xy}\right)_{i+1,j+1}-\left(P_{xy}\right)_{i-1,j+1}\right)-\left(\left(P_{xy}\right)_{i+1,j-1}-\left(P_{xy}\right)_{i-1,j-1}\right)}{8c^3}\right)+\frac{\left(P_{yy}\right)_{i,j-1}-2\left(P_{yy}\right)_{i,j}+\left(P_{yy}\right)_{i,j+1}}{c^2}\right)+q,$$
$$L_{4,c}\left(\overline{M}_{xx},\overline{M}_{xy}\right)=\frac{1}{2c}\left(\left(\overline{M}_{xx}\right)_{i+1,j}-\left(\overline{M}_{xx}\right)_{i-1,j}+\left(\overline{M}_{xy}\right)_{i,j+1}-\left(\overline{M}_{xy}\right)_{i,j-1}\right)-\overline{Q}_x,$$
$$L_{5,c}\left(\overline{M}_{xy},\overline{M}_{yy}\right)=\frac{1}{2c}\left(\left(\overline{M}_{xy}\right)_{i+1,j}-\left(\overline{M}_{xy}\right)_{i-1,j}+\left(\overline{M}_{yy}\right)_{i,j+1}-\left(\overline{M}_{yy}\right)_{i,j-1}\right)-\overline{Q}_y. \tag{32}$$

The obtained system of (31) with the supplemented boundary conditions equation and the initial conditions equation is solved by the fourth-order Runge-Kutta method. Figure 5 shows a comparison between the time responses of the system equations (4a), (4b), and (4c) using the Runge-Kutta of fourth-order method and the time response of the problems (31), using the finite difference method at the same values of the parameters shown in Figure 2.

4.2. Frequency Response Curves. When the amplitude achieves a constant nontrivial value, a steady-state vibration exists. Using the frequency response equations we can assess the influence of the damping coefficients, the nonlinear parameters, and the excitation amplitude on the steady-state amplitudes. The frequency response equations (24)–(29) are nonlinear equations in a_1, a_2, and a_3 which are solved numerically. The numerical results are shown in Figures 6–25, and in all figures the region of stability of the nonlinear solutions is determined by applying the Routh-Hurwitz criterion. The solid lines stand for the stable solution, and the dotted lines stand for the unstable solution. From the geometry of the figures, we observe that each curve is continuous and has stable and unstable solutions.

4.2.1. Response Curve of Case 1. To check the accuracy of the analytical solution derived by the multiple time scale in predicting the amplitude of the first mode, we compare the amplitude of the first mode obtained from frequency response equation of Case 1 with values obtained from numerical integration of (4a). Figure 6 shows a comparison of these outputs for the first mode. The effects of the detuning parameter σ_1 on the steady-state amplitude of the first mode for the stability first case, where $a_1 \neq 0$, $a_2 = 0$, and $a_3 = 0$, for the parameters $\mu_1 = 0.2$, $\alpha_7 = 0.01$, $\omega_1 = 2.3$, $f_1 = 4$, $f_{11} = 0.1$, $f_{12} = 0.2$, $f_{14} = 0.5$, $\Omega_1 = 1$, $\Omega_2 = 1.2$, and $\Omega_4 = 1.4$, as shown in Figure 6.

Figures 7–11, show the effects of the damping coefficient μ_1, the first mode natural frequency ω_1, the external

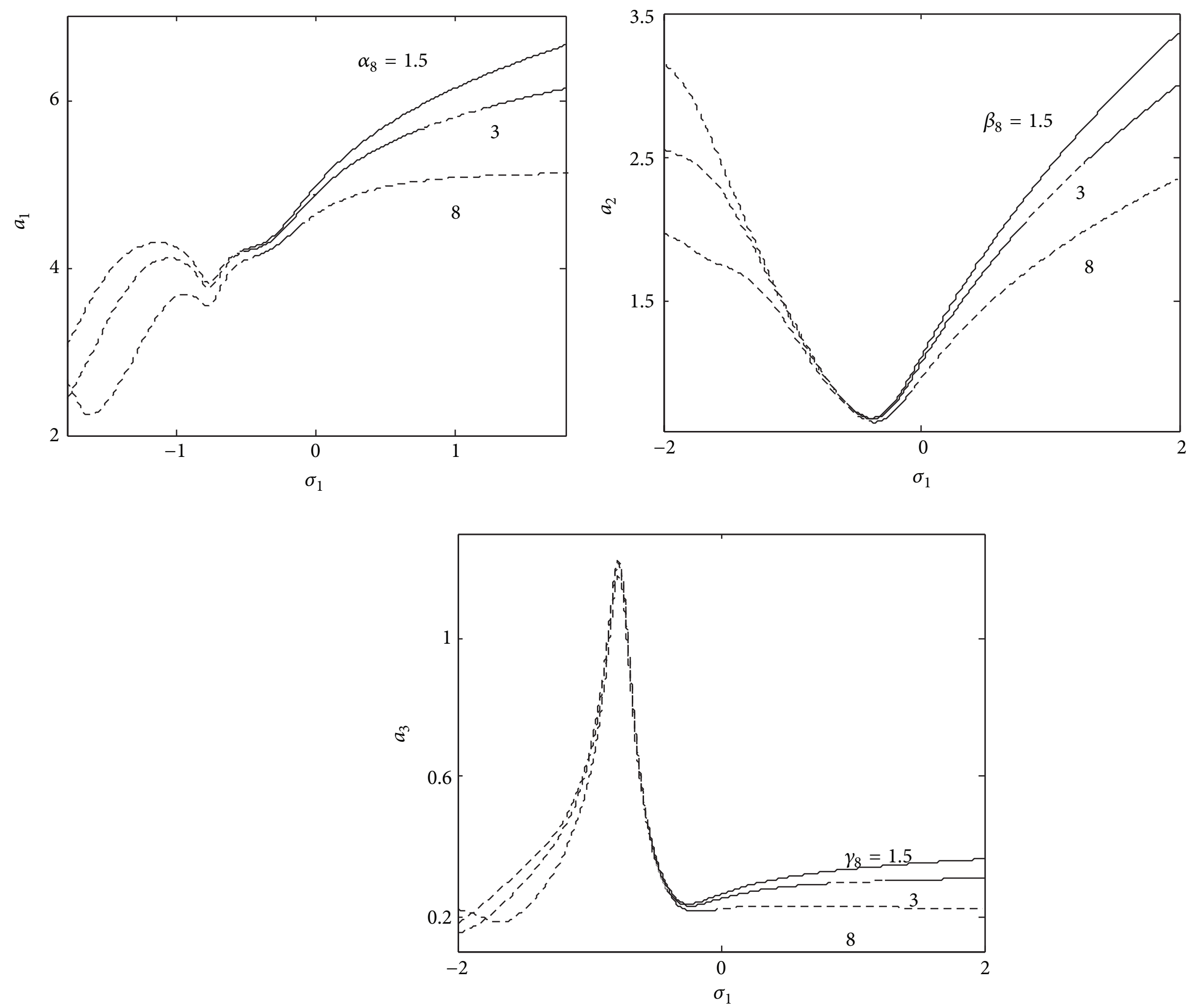

Figure 21: Effects of the nonlinear parameters (α_8, β_8, and γ_8 coupling terms).

excitation amplitude f_1, the nonlinear spring stiffness α_7, and the parametric excitation f_{14}. Figures 7 and 8 show that the steady-state amplitude a_1 is inversely proportional to μ_1 and ω_1, and also for decreasing μ_1 or ω_1 the curve is bending to the left. It is clear from Figure 9 that the steady-state amplitude a_1 is increasing for increasing value of external excitation force f_1, and the zone of instability is increased. Figure 10 shows that as the nonlinear spring stiffness α_7 is increased; the continuous curve is moved downwards. Also, the negative and positive values of α_7 produce either hard or soft spring, respectively, as the curve is either bent to the right or to the left, leading to the appearance of the jump phenomenon. The region of stability is increased for increasing value of α_7. From Figure 11, we observe that for increasing value of parametric excitation amplitude f_{14}, the steady-state amplitude of the first mode is increased, and the curve is shifted to the left.

4.2.2. Response Curve of Case 2. Figures 12–16, show the frequency response curves for the stability of the second case, where $a_2 \neq 0$, $a_1 = 0$, and $a_3 = 0$. Figure 12 shows a comparison of these outputs for the second mode. The effects of the detuning parameter σ_2 on the steady-state amplitude of the second mode for the stability second case, where $a_2 \neq 0$, $a_1 = 0$, $a_3 = 0$, for the parameters: $\mu_2 = 0.2$, $\beta_8 = 0.01$, $\omega_2 = 4$, $f_2 = 4$, $f_{21} = 0.1$, $f_{22} = 0.2$, $f_{24} = 0.5$, $\Omega_1 = 1$, $\Omega_2 = 1.2$, and $\Omega_4 = 1.4$, as shown in Figure 12. It can be seen from the figure that maximum steady-state amplitude occurs when $\omega_2 \cong \omega_1$. Figure 13 shows that as the nonlinear spring stiffness β_8 is increased, the continuous curve is moved downwards. Also, the positive and negative values of β_8 produce either soft or hard spring, respectively, as the curve is either bent to the left or to the right, leading to the appearance of the jump phenomenon. Figures 14, 15, and 16 show that the steady-state amplitude a_2 is inversely proportional to μ_2, ω_2 and directly proportional to the external excitation f_2. Also, for decreasing μ_2, ω_2 the curve is bending to the left.

4.2.3. Response Curve of Case 6. Figures 17, 18, 19, 20, 21, 22, 23, 24, and 25 show that the frequency response curves for practical case stability, where $a_1 \neq 0$, $a_2 \neq 0$, and $a_3 \neq 0$.

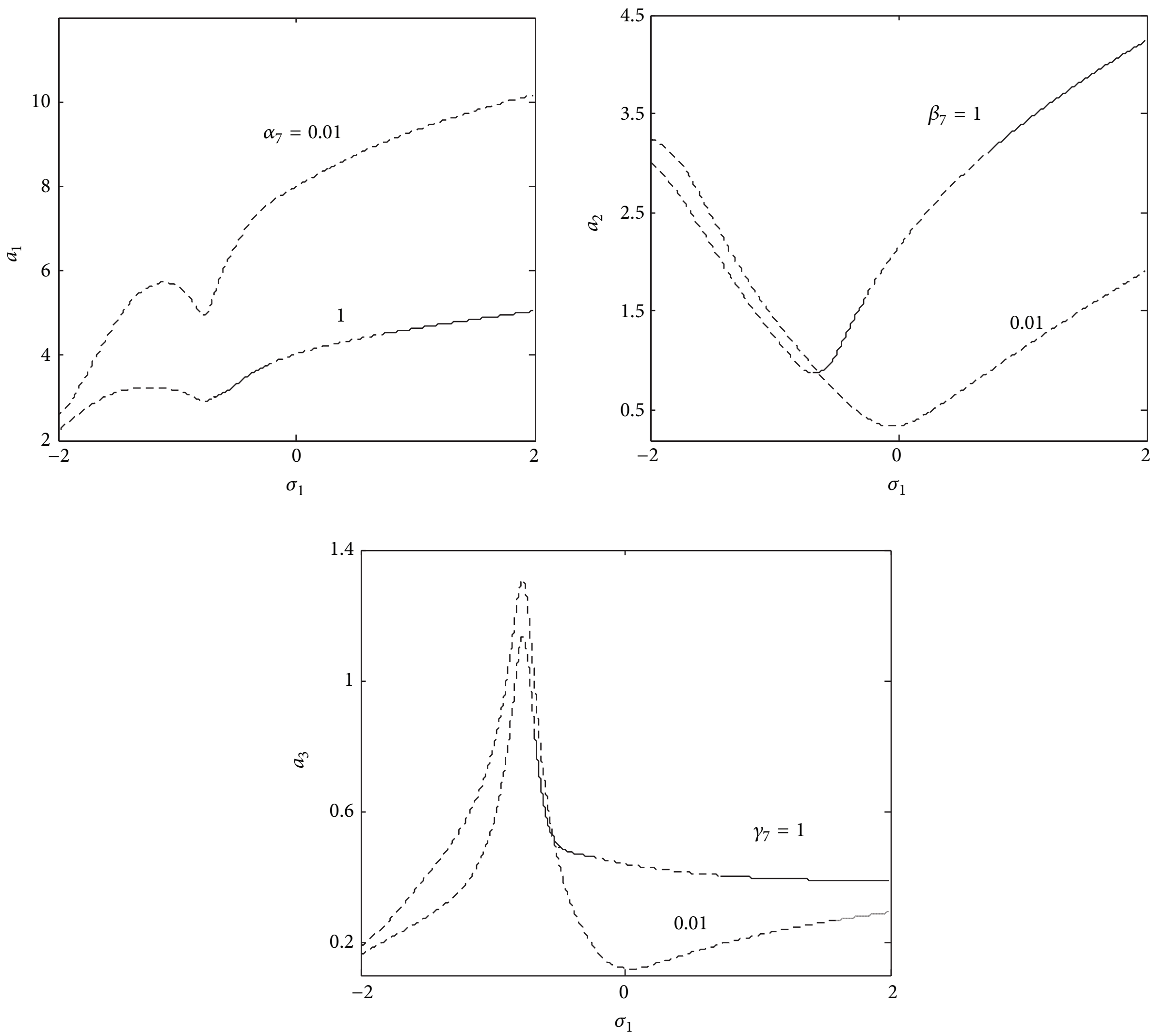

Figure 22: Effects of the nonlinear parameters (α_7, β_7, and γ_7 coupling terms).

Figure 17 shows that the effects of the detuning parameter σ_1 on the amplitudes of the three modes. From this figure, we observe that these modes intersect, and for positive value of the detuning parameter σ_1 the amplitudes are stable. For negative value of the detuning parameter σ_1 down to and including -0.5 the system becomes unstable.

Figure 18 shows that the steady-state amplitudes of the three modes a_1, a_2, and a_3 are directly proportional to the external excitation force f_1. Also, form this figure we show that the stability region is decreased for increasing f_1. Figures 19–21 show that the steady-state amplitudes and stability of the three modes a_1, a_2, and a_3 are inversely proportional to the nonlinear parameters $(\alpha_1, \alpha_2, \alpha_8)$, $(\beta_1, \beta_2, \beta_8)$, and $(\gamma_1, \gamma_2, \gamma_8)$, respectively.

Figures 22–24, show the effects of the nonlinear parameters $(\alpha_7, \beta_7, \gamma_7)$, $(\alpha_3, \beta_3, \gamma_3)$, and $(\alpha_5, \beta_5, \gamma_5)$ on the steady-state amplitudes of the three modes. It is clear that the stability regions are increased for increasing these nonlinear parameters. For increasing value of linear viscous damping coefficients, we note that the steady-state amplitudes are increasing or decreasing for the first, second, and third modes, respectively, as shown in Figure 25. The region of stability system is increased for decreasing value of damping coefficients.

4.3. Comparison Study. In the previous work [11], the chaotic dynamics of a six-dimensional nonlinear system which represents the averaged equation of a composite laminated piezoelectric rectangular plate subjected to the transverse, in-plane excitations and the excitation loaded by piezoelectric layers are analyzed. The case of 1 : 2 : 4 internal resonances is considered.

In our study, the nonlinear analysis and stability of a composite laminated piezoelectric rectangular thin plate under simultaneous external and parametric excitation forces

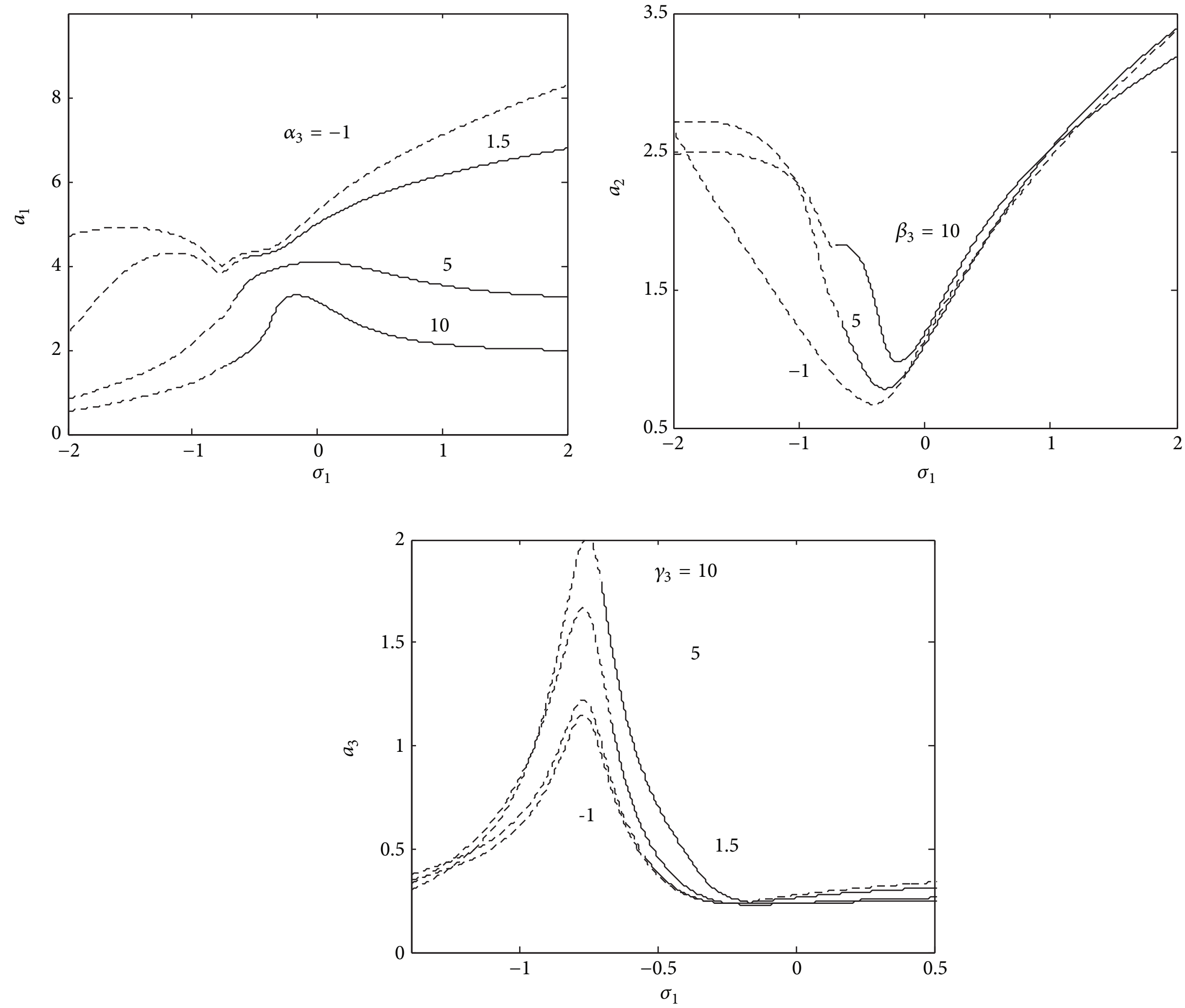

Figure 23: Effects of the nonlinear parameters (α_3, β_3, and γ_3 coupling terms).

are investigated. The second-order approximation is obtained to consider the influence of the cubic terms on nonlinear dynamic characteristics of the composite laminated piezoelectric rectangular plate using the multiple scale method. All possible resonance cases are extracted at this approximation order. The case of 1 : 1 : 3 internal resonance and primary resonance is considered. The stability of the system and the effects of different parameters on system behavior have been studied using phase plane and frequency response curves. The analytical results given by the method of multiple time scale are verified by comparison with results from numerical integration of the modal equations. Reliability of the obtained results is verified by comparison between the finite difference method (FDM) and Runge-Kutta method (RKM). Variation of the some parameters leads to multivalued amplitudes and hence to jump phenomena. It is quite clear that some of the simultaneous resonance cases are undesirable in the design of such system. Such cases should be avoided as working conditions for the system.

5. Conclusions

Multiple time scale perturbation method is applied to determine second-order approximate solutions for rectangular symmetric cross-ply laminated composite thin plate subjected to external and parametric excitations. Second-order approximate solutions are obtained to study the influence of the cubic terms on nonlinear dynamic characteristics of the composite laminated piezoelectric rectangular plate. All possible resonance cases are extracted at this approximation order. The study is focused on the case of 1 : 1 : 3 primary resonance and internal resonance, where $\Omega_3 \cong \omega_1$, $\omega_2 \cong \omega_1$, and $\omega_3 \cong 3\omega_1$. The analytical results given by the method of multiple time scale are verified by comparison with results from numerical integration of the modal equations. Reliability of the obtained results is verified by comparison between the finite difference method (FDM) and Runge-Kutta method (RKM). The stability of a composite laminated piezoelectric rectangular thin plate is investigated. The phase-plane

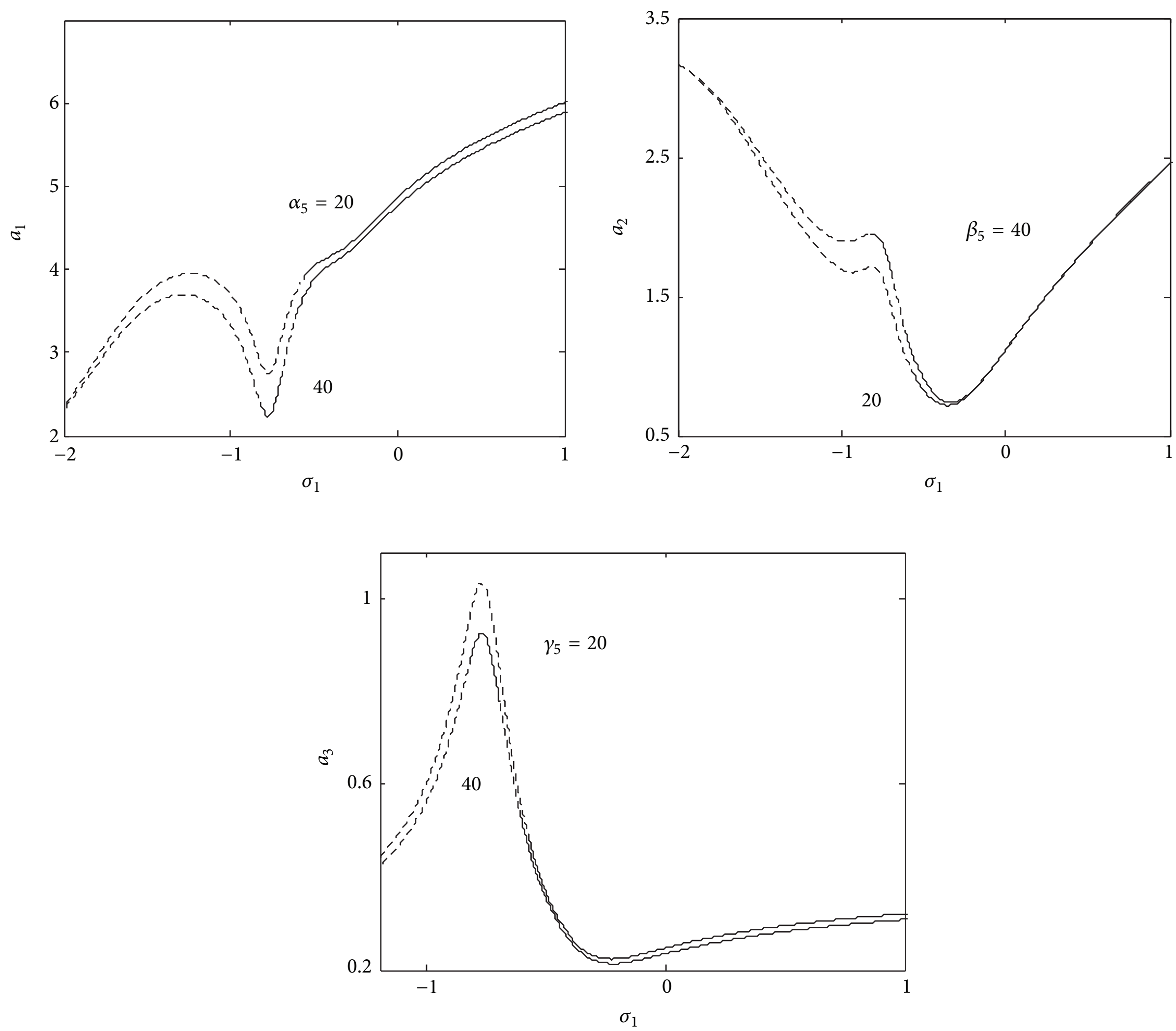

Figure 24: Effects of the nonlinear parameters (α_5, β_5, and γ_5 coupling terms).

method and frequency response curves are applied to study the stability of the system. From the previous study the following may be concluded.

(1) The simultaneous resonance case $\Omega_3 \cong \omega_1$, $\omega_2 \cong \omega_1$, and $\omega_3 \cong 3\omega_1$ is one of the worst case, and they should be avoided in design of such system. Of course, the excitation frequency Ω_3 is out of control. But this case should be avoided through having $\omega_2 \neq \omega_1$ or $\omega_3 \neq 3\omega_1$.

(2) A comparison between the solutions obtained numerically with that prediction from the multiple scales shows an excellent agreement.

(3) Reliability of the obtained results is verified by comparison between the finite difference method (FDM) and Runge-Kutta method (RKM).

(4) Variation of the parameters μ_1, μ_2, α_7, β_8, ω_1, ω_2, f_1, f_2 leads to multivalued amplitudes and hence to jump phenomena.

(5) For the first and second modes, the steady-state amplitudes a_1 and a_2 are directly proportional to the excitation amplitude f_1 and f_2 and inversely proportional to the linear damping μ_1 and μ_2, respectively.

(6) The negative and positive values of nonlinear stiffness α_7, β_8 produce either hard or soft spring, respectively, as the curve is either bent to the right or to the left.

(7) The region of instability increase, which is undesirable, for increasing excitation amplitudes f_1, f_2 and for negative values of nonlinear stiffness α_7, β_8.

(8) The multivalued solutions are disappeared for increasing linear damping coefficients μ_1, μ_2.

(9) The region of stability increases, which is desirable for decreasing excitation amplitude f_1, nonlinear parameters $(\alpha_1, \beta_1, \gamma_1)$, $(\alpha_2, \beta_2, \gamma_2)$, and for increasing nonlinear stiffness $(\alpha_7, \beta_7, \gamma_7)$.

(10) The steady-state amplitudes of the three modes a_1, a_2, and a_3 are directly proportional to the excitation amplitude f_1 and inversely proportional to

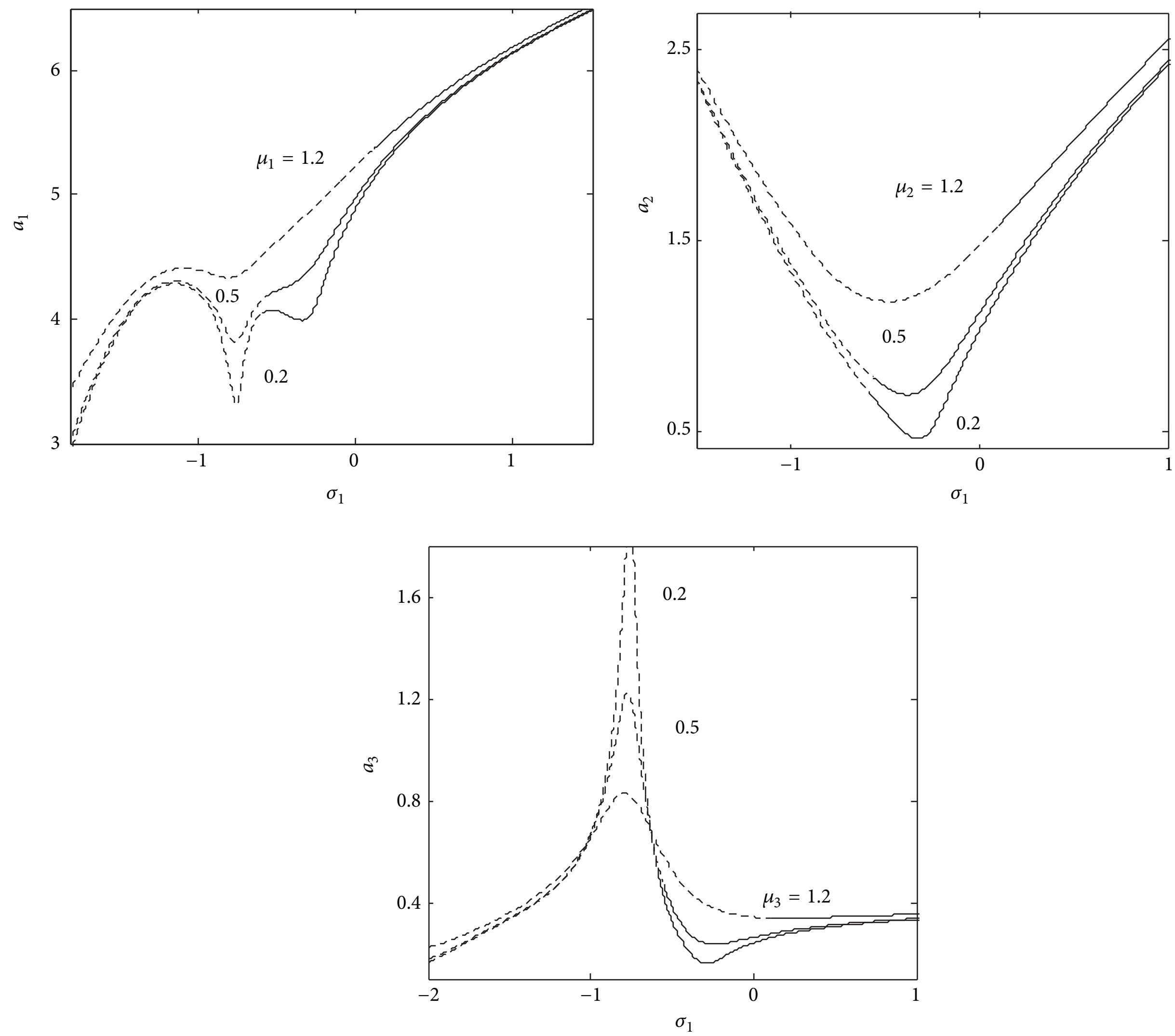

FIGURE 25: Effects of the linear damping coefficients.

the nonlinear parameters $(\alpha_1, \alpha_2, \alpha_8)$, $(\beta_1, \beta_2, \beta_8)$, and $(\gamma_1, \gamma_2, \gamma_8)$, respectively.

For further work, we intend to extend our work to explore the modeling formulation by investigating the role static loading (in addition to the dynamic component).

Acknowledgment

The authors would like to thank the anonymous reviewers for their valuable comments and suggestions for improving the quality of this paper.

References

[1] M. Ye, J. Lu, W. Zhang, and Q. Ding, "Local and global nonlinear dynamics of a parametrically excited rectangular symmetric cross-ply laminated composite plate," *Chaos, Solitons & Fractals*, vol. 26, no. 1, pp. 195–213, 2005.

[2] W. Zhang, "Global and chaotic dynamics for a parametrically excited thin plate," *Journal of Sound and Vibration*, vol. 239, no. 5, pp. 1013–1036, 2001.

[3] X. Y. Guo, W. Zhang, and M. Yao, "Nonlinear dynamics of angle-ply composite laminated thin plate with third-order shear deformation," *Science China Technological Sciences*, vol. 53, no. 3, pp. 612–622, 2010.

[4] W. Zhang, Z. Liu, and P. Yu, "Global dynamics of a parametrically and externally excited thin plate," *Nonlinear Dynamics*, vol. 24, no. 3, pp. 245–268, 2001.

[5] W. M. Tien, N. S. Namachchivaya, and A. K. Bajaj, "Nonlinear dynamics of a shallow arch under periodic excitation-I. 1:2 internal resonance," *International Journal of Non-Linear Mechanics*, vol. 29, no. 3, pp. 349–366, 1994.

[6] M. Sayed and A. A. Mousa, "Second-order approximation of angle-ply composite laminated thin plate under combined excitations," *Communications in Nonlinear Science and Numerical Simulation*, vol. 17, no. 12, pp. 5201–5216, 2012.

[7] W. Zhang, C. Song, and M. Ye, "Further studies on nonlinear oscillations and chaos of a symmetric cross-ply laminated thin

plate under parametric excitation," *International Journal of Bifurcation and Chaos in Applied Sciences and Engineering*, vol. 16, no. 2, pp. 325–347, 2006.

[8] W. Zhang, J. Yang, and Y. Hao, "Chaotic vibrations of an orthotropic FGM rectangular plate based on third-order shear deformation theory," *Nonlinear Dynamics*, vol. 59, no. 4, pp. 619–660, 2010.

[9] W. Zhang, Z. Yao, and M. Yao, "Periodic and chaotic dynamics of composite laminated piezoelectric rectangular plate with one-to-two internal resonance," *Science in China, Series E*, vol. 52, no. 3, pp. 731–742, 2009.

[10] W. Zhang and S. B. Li, "Resonant chaotic motions of a buckled rectangular thin plate with parametrically and externally excitations," *Nonlinear Dynamics*, vol. 62, no. 3, pp. 673–686, 2010.

[11] W. Zhang, M. Gao, M. Yao, and Z. Yao, "Higher-dimensional chaotic dynamics of a composite laminated piezoelectric rectangular plate," *Science in China, Series G*, vol. 52, no. 12, pp. 1989–2000, 2009.

[12] W. Zhang and W. L. Hao, "Multi-pulse chaotic dynamics of six-dimensional non-autonomous nonlinear system for a composite laminated piezoelectric rectangular plate," *Nonlinear Dynamics*, 2013.

[13] X. Y. Guo and W. Zhang, "Nonlinear dynamics of composite laminated thin plate with 1:2:3 inner resonance," in *Proceedings of the 2nd International Conference on Mechanic Automation and Control Engineering (MACE '11)*, pp. 7479–7482, July 2011.

[14] M. Eissa and M. Sayed, "A comparison between active and passive vibration control of non-linear simple pendulum. I.," *Mathematical & Computational Applications*, vol. 11, no. 2, pp. 137–149, 2006.

[15] M. Eissa and M. Sayed, "A comparison between active and passive vibration control of non-linear simple pendulum. II. Longitudinal tuned absorber and negative $G\ddot{\varphi}$ and $G\varphi^n$ feedback," *Mathematical & Computational Applications*, vol. 11, no. 2, pp. 151–162, 2006.

[16] M. Eissa and M. Sayed, "Vibration reduction of a three DOF non-linear spring pendulum," *Communications in Nonlinear Science and Numerical Simulation*, vol. 13, no. 2, pp. 465–488, 2008.

[17] M. Sayed, *Improving the mathematical solutions of nonlinear differential equations using different control methods [Ph.D. thesis]*, Menoufia University, Menoufia, Egypt, 2006.

[18] M. Sayed and M. Kamel, "Stability study and control of helicopter blade flapping vibrations," *Applied Mathematical Modelling*, vol. 35, no. 6, pp. 2820–2837, 2011.

[19] M. Sayed and M. Kamel, "1:2 and 1:3 internal resonance active absorber for non-linear vibrating system," *Applied Mathematical Modelling*, vol. 36, no. 1, pp. 310–332, 2012.

[20] M. Sayed and Y. S. Hamed, "Stability and response of a nonlinear coupled pitch-roll ship model under parametric and harmonic excitations," *Nonlinear Dynamics*, vol. 64, no. 3, pp. 207–220, 2011.

[21] Y. A. Amer, H. S. Bauomy, and M. Sayed, "Vibration suppression in a twin-tail system to parametric and external excitations," *Computers and Mathematics with Applications*, vol. 58, no. 10, pp. 1947–1964, 2009.

[22] Y. S. Hamed, M. Sayed, D.-X. Cao, and W. Zhang, "Nonlinear study of the dynamic behavior of a string-beam coupled system under combined excitations," *Acta Mechanica Sinica*, vol. 27, no. 6, pp. 1034–1051, 2011.

[23] J. Awrejcewicz, V. A. Krysko, I. V. Papkova, and A. V. Krysko, "Routes to chaos in continuous mechanical systems. Part 1: mathematical models and solution methods," *Chaos, Solitons & Fractals*, vol. 45, pp. 687–708, 2012.

[24] A. V. Krysko, J. Awrejcewicz, I. V. Papkova, and V. A. Krysko, "Routes to chaos in continuous mechanical systems. Part 2: modelling transitions from regular to chaotic dynamics," *Chaos, Solitons & Fractals*, vol. 45, pp. 709–720, 2012.

[25] J. Awrejcewicz, A. V. Krysko, I. V. Papkova, and V. A. Krysko, "Routes to chaos in continuous mechanical systems. Part 3: the Lyapunov exponents, hyper, hyper-hyper and spatial-temporal chaos," *Chaos, Solitons & Fractals*, vol. 45, pp. 721–736, 2012.

[26] J. Awrejcewicz, A. V. Krysko, J. Mrozowski, O. A. Saltykova, and M. V. Zhigalov, "Analysis of regular and chaotic dynamics of the Euler-Bernoulli beams using finite difference and finite element methods," *Acta Mechanica Sinica*, vol. 27, no. 1, pp. 36–43, 2011.

[27] J. N. Reddy, "A refined nonlinear theory of plates with transverse shear deformation," *International Journal of Solids and Structures*, vol. 20, no. 9-10, pp. 881–896, 1984.

[28] Z. G. Yao, W. Zhang, and L. H. Chen, "Periodic and chaotic oscillations of laminated composite piezoelectric rectangular plate with 1:2:3 internal resonances," in *Proceedings of the 5th International Conference on Nonlinear Mechanics*, pp. 720–725, Shanghai, China, 2007.

[29] A. H. Nayfeh, *Introduction to Perturbation Techniques*, Wiley-Interscience, New York, NY, USA, 1981.

[30] A. H. Nayfeh, *Nonlinear Interactions: Analytical, Computational, and Experimental Methods*, Wiley Series in Nonlinear Science, Wiley-Interscience, New York, NY, USA, 2000.

[31] A. H. Nayfeh, *Perturbation Methods*, John Wiley & Sons, New York, NY, USA, 1973.